

AD-A245 999



**NAVAL POSTGRADUATE SCHOOL**  
**Monterey, California**



**DTIC**  
**SELECTE**  
**FEB 18 1992**  
**S B D**

**THESIS**

**MULTIPLE-WAVELENGTH  
TRANSMISSION MEASUREMENTS  
IN ROCKET MOTOR PLUMES**

by

Hong-on Kim

September, 1991

Thesis Advisor:  
Co-Advisor:

David W. Netzer  
David Laredo

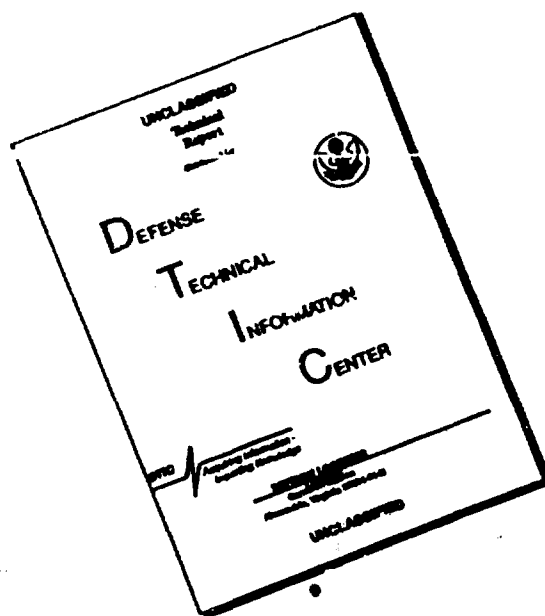
Approved for public release; distribution is unlimited

**92 2 12 156**

**92-03676**



# DISCLAIMER NOTICE



**THIS DOCUMENT IS BEST  
QUALITY AVAILABLE. THE COPY  
FURNISHED TO DTIC CONTAINED  
A SIGNIFICANT NUMBER OF  
PAGES WHICH DO NOT  
REPRODUCE LEGIBLY.**

UNCLASSIFIED

SECURITY CLASSIFICATION OF THIS PAGE

REPORT DOCUMENTATION PAGE				
1a REPORT SECURITY CLASSIFICATION Unclassified			1b RESTRICTIVE MARKINGS	
2a SECURITY CLASSIFICATION AUTHORITY			3 DISTRIBUTION/AVAILABILITY OF REPORT Approved for public release; distribution is unlimited.	
2b DECLASSIFICATION/DOWNGRADING SCHEDULE				
4 PERFORMING ORGANIZATION REPORT NUMBER(S)			5 MONITORING ORGANIZATION REPORT NUMBER(S)	
6a NAME OF PERFORMING ORGANIZATION Naval Postgraduate School		6b OFFICE SYMBOL (If applicable) 55		7a NAME OF MONITORING ORGANIZATION Naval Postgraduate School
6c ADDRESS (City, State, and ZIP Code) Monterey, CA 93943-5000			7b ADDRESS (City, State, and ZIP Code) Monterey, CA 93943-5000	
8a NAME OF FUNDING/SPONSORING ORGANIZATION Air Force Phillips Laboratory		8b OFFICE SYMBOL (If applicable)		9 PROCUREMENT INSTRUMENT IDENTIFICATION NUMBER
8c ADDRESS (City, State, and ZIP Code)  Edwards AFB, CA 93523-5000			10 SOURCE OF FUNDING NUMBERS	
			Program Element No	Project No
			Task No F0461191X004	Work Unit Accession Number
11 TITLE (Include Security Classification) MULTIPLE-WAVELENGTH TRANSMISSION MEASUREMENTS IN ROCKET MOTOR PLUMES				
12 PERSONAL AUTHOR(S) Kim, Hong-on				
13a TYPE OF REPORT Master's Thesis		13b TIME COVERED From To		14. DATE OF REPORT (year, month, day) 1991, September
15 PAGE COUNT 63				
16 SUPPLEMENTARY NOTATION The views expressed in this thesis are those of the author and do not reflect the official policy or position of the Department of Defense or the U.S. Government.				
17 COSATI CODES			18 SUBJECT TERMS (continue on reverse if necessary and identify by block number)	
FIELD	GROUP	SUBGROUP		
			Solid -Propellant; Rocket Motor; Light Transmission; Particle Sizing	
19 ABSTRACT (continue on reverse if necessary and identify by block number)  Multiple-wavelength light transmission measurements were used to measure the mean particle size (d32), index of refraction (m) and standard deviation of the small particles in the edge of the plume of a small solid propellant rocket motor. The results have shown that the multiple-wavelength light transmission measurement technique can be used to obtain these variables. The technique was shown to be more sensitive to changes in d32 and standard deviation than to m. A GAP/AP/4.7 % aluminum propellant burned at 25 atm produced particles with d32 = 0.150 +/- 0.006 microns, standard deviation = 1.50 +/- 0.04 and m = 1.63 +/- 0.13. The good correlation of the data indicated that only submicron particles were present in the edge of the plume.				
20 DISTRIBUTION/AVAILABILITY OF ABSTRACT <input checked="" type="checkbox"/> UNCLASSIFIED/UNLIMITED <input type="checkbox"/> SAME AS REPORT <input type="checkbox"/> DTIC USERS			21 ABSTRACT SECURITY CLASSIFICATION Unclassified	
22a NAME OF RESPONSIBLE INDIVIDUAL Prof. David W. Netzer			22b TELEPHONE (Include Area code) (408) 646-2980	
			22c OFFICE SYMBOL Code AA/Nt	

DD FORM 1473, 84 MAR

83 APR edition may be used until exhausted  
All other editions are obsolete

SECURITY CLASSIFICATION OF THIS PAGE

Approved for public release; distribution is unlimited.

Multiple-Wavelength Transmission Measurements  
in Rocket Motor Plumes

by

Kim, Hong-on  
Major, Korean Air Force  
B.S., Korean Air Force Academy

Submitted in partial fulfillment  
of the requirements for the degree of

MASTER OF SCIENCE IN AERONAUTICAL ENGINEERING

from the

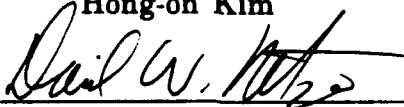
NAVAL POSTGRADUATE SCHOOL  
September, 1991

Author:

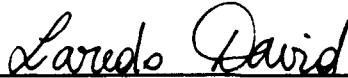


Hong-on Kim

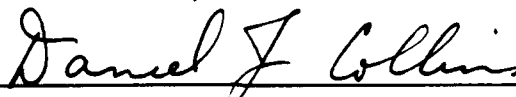
Approved by:



David W. Netzer, Thesis Advisor



David Laredo, Second Reader



Daniel J. Collins, Chairman

Department of Aeronautics and Astronautics

## ABSTRACT

Multiple-wavelength light transmission measurements were used to measure the mean particle size ( $d_{32}$ ), index of refraction ( $m$ ) and standard deviation ( $\sigma$ ) of the small particles in the edge of the plume of a small solid propellant rocket motor. The results have shown that the multiple-wavelength light transmission measurement technique can be used to obtain these variables. The technique was shown to be more sensitive to changes in  $d_{32}$  and standard deviation ( $\sigma$ ) than to  $m$ . A GAP/AP/4.7 % aluminum propellant burned at 25 atm produced particles with  $d_{32} = 0.150 \pm 0.006 \mu$ ,  $\sigma = 1.50 \pm 0.04$  and  $m = 1.63 \pm 0.13$ . The good correlation of the data indicated that only submicron particles were present in the edge of the plume.

Accession For	
NTIS GRA&I	<input checked="checked" type="checkbox"/>
DTIC TAB	<input type="checkbox"/>
Unannounced	<input type="checkbox"/>
Justification	
By	
Distribution/	
Availability Codes	
Dist	Avail and/or Special
A-1	

## TABLE OF CONTENTS

I. INTRODUCTION .....	1
II. THEORETICAL BACKGROUND .....	4
III. EXPERIMENTAL APPARATUS .....	7
A. ROCKET MOTOR .....	7
B. LIGHT TRANSMITTANCE APPARATUS .....	9
C. DATA ACQUISITION AND REDUCTION .....	11
IV. RESULTS AND DISCUSSION .....	17
A. INTRODUCTION .....	17
B. SYSTEM CALIBRATION .....	18
C. ROCKET MOTOR PLUME DATA .....	18
V. CONCLUSIONS AND RECOMMENDATIONS .....	40
APPENDICES .....	41
A. DIODE READINGS .....	41
B. DATA ACQUISITION PROGRAM .....	47

REFERENCES .....	50
------------------	----

INITIAL DISTRIBUTION LIST .....	52
---------------------------------	----

## LIST OF FIGURES

III-1.	Photograph of the Motor Components . . . . .	13
III-2.	Photograph of Installed Rocket Motor . . . . .	13
III-3.	Photograph of Light Transmittance System . . . . .	14
III-4.	Schematic Diagram of Light Transmittance Apparatus . . . . .	15
III-5.	Spectral Irradiance of the Hg Lamp . . . . .	16
III-6.	Diode Spectral Response . . . . .	16
IV-1.	Configurations of the Motor and Plume . . . . .	19
IV-2.	Voltage vs. Diode Number Run 1 without Plume . . . . .	26
IV-3.	Voltage vs. Diode Number, Run 1, in Plume . . . . .	27
IV-4.	Voltage vs. Diode Number, Run 2, without Plume . . . . .	28
IV-5.	Voltage vs. Diode Number, Run 2, in Plume . . . . .	29
IV-6.	Voltage vs. Diode Number, Run 3, without Plume . . . . .	30
IV-7.	Voltage vs. Diode Number, Run 3, in Plume . . . . .	31
IV-8.	Extinction Coefficients . . . . .	32
IV-9.	Extinction Coefficient Ratios . . . . .	33
IV-10.	Iteration Flow Scheme . . . . .	34
IV-11.	Data Correlation Sensitivity for Specified $D_{32}$ , Run 1 . . . . .	35
IV-12.	Data Correlation Sensitivity for Specified $\sigma$ , Run 1 . . . . .	36
IV-13.	Data Correlation Sensitivity for Specified $m$ , Run 1 . . . . .	37



IV-14. Log Transmission vs. Extinction Coefficient Ratios, Run 1,2 & 3 . . . . .	38
IV-15. Log Transmission vs. Extinction Coefficient Ratios, Including 0.6328 $\mu$ Laser Data, Run 3 . . . . .	39

## LIST OF TABLES

III-1. NOZZLE SPECIFICATIONS .....	8
III-2. LIGHT SPECIFICATIONS .....	9
III-3. MULTISPEC SPECIFICATIONS .....	10
IV-1. SUMMARY OF MOTOR FIRINGS .....	19
IV-2. DIODE READINGS AND TRANSMITTANCE .....	21
IV-3. LOG TRANSMISSION RATIOS .....	21
IV-4. REGRESSION ANALYSIS FOR THE RUNS .....	23
IV-5. ESTIMATES OF MEASUREMENT ACCURACY, RUN 2 .....	25

## **ACKNOWLEDGEMENTS**

I would like to offer my most sincere thanks and appreciation to Prof. David W. Netzer for giving me the opportunity to work with him on this project. There are no words to describe his support and guidance during the research period. I'm similarly grateful to Dr. David Laredo whose expertise in this area was invaluable. I would also like to thank the Aeronautical Engineering technical staff for their assistance in making the necessary apparatus.

Finally, Thanks to my wife, Myoung-sook, and my lovely daughter, Jee-youn, for their support and understanding.

## I. INTRODUCTION

In today's budget conscious industry, the solid propellant rocket motor is an ideal propulsion system due to its low cost and simplicity. The major obstacle for solid rocket motors, however, is their limited specific impulse compared to airbreathing motors. One way to help overcome this limitation is to utilize metal fuel additives. Solid propellant rocket motors can achieve high specific impulse with metal fuel additives such as aluminum. Aluminum propellants also increase propellant densities and suppress transverse modes of combustion oscillations by damping the oscillations with the aluminum agglomerates in the combustion chamber. One disadvantage of using metal fuel additives that cause large agglomerates in a rocket motor is a large thrust loss. The agglomerates remain as relatively large condensed particles in the nozzle expansion process, resulting in velocity and thermal lags between the condensed particles and the expanding gas. Additional losses occur due to the fact that, unlike a gas, the condensed particles do not expand in the nozzle expansion area. These losses, called two phase flow losses, are often the largest factor in the determination of the nozzle loss coefficient [Ref. 1]. Besides causing performance losses in the nozzle, the condensed  $\text{Al}_2\text{O}_3$  particles are the major source of primary smoke in the exhaust plume. This has significance when missiles are designed for tactical purposes and plume signature is a critical issue. The particulate matter can also have major effects upon the plume IR signature. High number densities of particles can block gas-phase radiation from the plume. They can also be the

source of radiation, especially the larger particles which exit the nozzle not in thermal equilibrium with the gas. The detection, identification, tracking and targeting of missiles that employ these propellants are all important issues in the development of space defence systems.

The prediction of plume signature is currently accomplished using codes such as SPF and SIRRUM [Ref. 2]. The nozzle/plume flowfield codes [Ref. 2, 3] predict that the particle size distribution within the plume is not uniformly distributed in the radial direction. Particles larger than approximately  $3\mu$  are concentrated along the plume centerline, failing to follow the rapid gas flow turning that occurs in the nozzle throat region. Even particles as small as  $1\mu$  are predicted not to follow the flow along the diverging nozzle wall. Thus, it is expected that particles in the outer regions of the plume will be less than  $1\mu$  in diameter.

The particle size distribution, particle composition and particle optical properties all have considerable influence on the plume signature. Both the prediction of plume signature and the measurement of particle size distributions within the plume depend upon an accurate knowledge of the particle optical properties, especially the particle complex refractive index. For aluminum oxide the refractive index is generally believed to be between 1.65 and 1.85, whereas the absorption coefficient has been reported to be between  $10^{-2}$  and  $10^{-7}$  [Ref. 4]. Small amounts of contaminants can apparently have a significant effect on the refractive index. This is of importance in rocket motor plumes since contaminants such as soot are present and the rapidly changing temperatures can result in various phases of aluminum oxide being present.

Larger booster motors use propellants with 14-20 % aluminum by weight, resulting in 25-38 % of the exhaust being condensed  $\text{Al}_2\text{O}_3$ . These plumes are very opaque, making optically based particle sizing diagnostic techniques difficult to employ.

The objective of the present investigation was to measure the mean particle size and particle index of refraction in the plume of a small solid propellant rocket motor which utilized a propellant with 4.7 % aluminum. The technique employed was multiple-wavelength light transmission measurements together with the use of Mie code for obtaining the mean extinction coefficients as a function of the particle size distribution, index of refraction and wavelengths of the illumination source. This technique is limited to particles smaller than approximately  $1.0 \mu$  [Ref. 5]. For this reason and the high plume opacity, the measurements were made within the edges of the plume. A collimated mercury light source was used to provide five distinct wavelengths for use with a spectrograph. A helium-neon laser was also used. Measurement sensitivity to the experimental variables was also investigated.

## II. THEORETICAL BACKGROUND

The light transmittance technique incorporates the use of multiple-wavelengths of light for continuous transmittance measurements through an exhaust plume containing particles. The values of transmittance are ratioed to each other and the mean particle size ( $d_{32}$ ) can then be calculated from the Mie theory, which describes the complex light scattering phenomena [Ref. 6].

This procedure was successfully applied by K. L. Cashdollar to measure the mass concentration and particle size of a cloud of smoke as discussed below [Ref. 5]. The transmission of light through a cloud of uniform particles is given by Bouguer's law:

$$T = \exp(-QAnL) = \exp\left[-\frac{3QC_m L}{2\rho d}\right] \quad (1)$$

where  $T$  = the fraction of light transmitted,

$Q$  = the dimensionless extinction coefficient,

$A$  = the cross sectional area of a particle,

$n$  = the number concentration of particles,

$L$  = the path length containing particles,

$C_m$  = the mass concentration of particles,

$\rho$  = the density of an individual particle, and

$d$  = the particle diameter.

Mie scattering theory for single spherical particle can be used to calculate the extinction coefficient ( $Q$ ) as a function of particle size, wavelength of light and complex refractive index of the particle. For polydisperse systems of particles, Dobbins [Ref. 7] showed that Bouguer's transmission law could be written in terms of mean properties :

$$T = \exp \left[ - \frac{3 \bar{Q} C_m L}{2 \rho d_{32}} \right] \quad (2)$$

where  $\bar{Q}$  = mean extinction coefficient

$d_{32}$  = the volume-to-surface mean particle diameter.

Equation (2) can be put into a more useful format by taking the natural log of both sides.

$$\ln T = \bar{Q} \left( - \frac{3 C_m L}{2 \rho d_{32}} \right) \quad (3)$$

Multi-wavelength transmission measurements are made over identical path lengths through the exhaust plume. The ratios of the logarithm of the transmissions at any two wavelength is thus equal to the ratio of the calculated mean extinction coefficients for the same wavelengths [Ref. 5].

$$\left( \frac{\ln T(\lambda_i)}{\ln T(\lambda_j)} \right)_{\text{experimental}} = \left( \frac{\bar{Q}(\lambda_i, d_{32})}{\bar{Q}(\lambda_j, d_{32})} \right)_{\text{theoretical}} \quad (4)$$

The transmittances are found experimentally. A computer program provided by K. L. Cashdollar [Ref. 5] was used to generate the mean extinction coefficients ( $\bar{Q}$ ) and the



extinction coefficient ratios ( $\bar{Q}(\lambda_1)/\bar{Q}(\lambda_2)$ ) versus  $d_{32}$ . These calculations were made for various values of the complex refractive index ( $m$ ) of the particle and the standard deviation ( $\sigma$ ) of the assumed log-normal particle size distribution. If the complex refractive index and standard deviation are correct, all the ratios would yield the same particle size ( $d_{32}$ ) within experimental measurement accuracy.

If the size of the submicron particles thought to be present in the edges of the plume can be assumed to obey a log-normal distribution, then there are four variables which must be determined;  $d_{32}$ ,  $\sigma$ , and the real and imaginary parts of the index of refraction. The latter was assumed independent of  $\lambda$ . Calculations with the Mie code showed that  $\bar{Q}$  was insensitive to the absorption index for the expected values between  $10^{-2}$  and zero. Thus, for transmission measurements, the aluminum oxide particles were assumed to have no absorption index. This resulted in the need for a minimum of three independent log-transmission ratios to determine  $d_{32}$ ,  $\sigma$  and the refractive index ( $m$ ).

### III. EXPERIMENTAL APPARATUS

#### A. ROCKET MOTOR

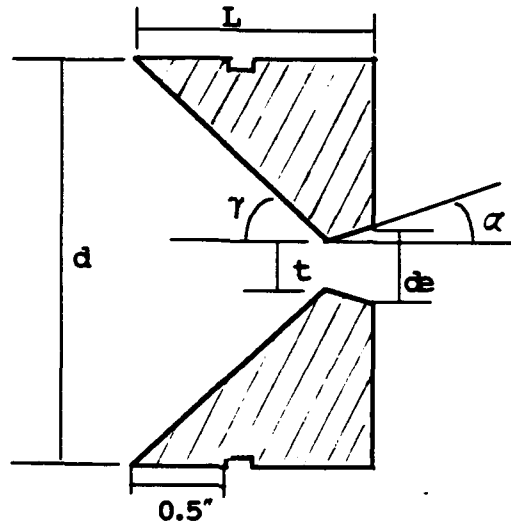
The rocket motor used in this experiment had the same internal dimensions as the long motor described by Rosa [Ref. 8]. The exterior of the motor was modified to remove the windows and make the outside diameter smaller. The motor components are displayed in a photograph in Figure III-1, and the installed motor is shown in Figure III-2.

An end-burning propellant grain was used with a 2" diameter and 1" web. The propellant was provided by the Air Force Philips Laboratory and was a GAP/AP propellant containing 4.7% aluminum. Motor ignition was accomplished using a small  $\text{BKNO}_3$  igniter located near the head-end of the motor. A disposable 1000 psi burst disk was installed to reduce the potential for motor over-pressurization. A single pressure port was located in the combustion chamber. The pressure port was connected to a Teledyne 0 ~ 1000 psi pressure transducer.

The outside dimensions of the motor chamber were approximately 10.5" in length by 3.25" in diameter. During actual motor loading, propellant surfaces in contact with motor walls were coated with commercially available 732-RTV self-vulcanizing silicone rubber to provide a burning inhibitor and to maintain propellant position in the motor.

The specifications and schematic of the nozzle are shown in TABLE III-1.

TABLE III-1. NOZZLE SPECIFICATIONS



	Description	Copper Nozzle
1	Outside Diameter (d)	2.12 inches
2	Length (L)	1.24 inches
3	Throat Diameter (t)	0.200 inches
4	Exit Diameter ( $d_e$ )	0.381 inches
5	Converging half-angle ( $\gamma$ )	45.0 degrees
6	Diverging half-angle ( $\alpha$ )	15.0 degrees

## B. LIGHT TRANSMITTANCE APPARATUS

The complete light scattering equipment with rocket motor in place is shown in Figure III-3. The overall arrangement of the light systems is seen in the photograph. The light sources used were a mercury lamp and a helium-neon laser. The cross pattern was used so that both light sources would penetrate the same path length in approximately the same plume location. Specifications are given in TABLEs III-2 and III-3.

The light scattering apparatus is depicted schematically in Figure III-4. The collimated white light beam was provided by a 100W Hg lamp (Oriel Model 6281). The ten distinct wavelengths produced by the mercury lamp are presented in Figure III-5 [Ref. 9]. The light transmitted through the plume entered a fixed input slit (Oriel Model 77220) which was 25  $\mu$  wide and 3 mm high, and fell upon the optics inside the Oriel

TABLE III-2. LIGHT SPECIFICATIONS

	White Light Source	He-Ne Laser
Manufacturer	Oriel	Spectra Physics
Model	6281	147
Type	Mercury Arc	He-Ne CW
Output Power	-	8 mW
Beam Diameter	-	0.92 mm
Wavelength	0.365, 0.4047, 0.4358, 0.5461, 0.577 $\mu$	.6328 $\mu$

TABLE III-3. MULTISPEC SPECIFICATIONS

Design	Crossed Czerny-Turner
F number	3.7
Focal length	125 mm
Grating type	Plane (Holographic)
Grating mount	Kinematic
Drive	Micrometer (Calibrated)
Optical Axis Height	1.78 in (45.2 mm)
Dimension	6×6×3 inch (150×150×80 mm)
Weight	3.3 lbs (1.5 kg)

MultiSpec spectrograph (Model 77400). MultiSpec was designed to be compatible with linear diode array detectors, and has a flat focal field for use with diode arrays up to 1 inch (25 mm) long. This instrument has a low F-number of 3.7, a focal length of 125 mm, a grating (Model 77420) with a spectral range of 250–800 nm, and a flat focal field. Gratings are selected to permit use of the wavelength band of interest. The photodiode array employed was a Reticon G-series solid state scanning device consisting of 1024 photodiodes on 25 micron centers. The response characteristics of the diode are presented in Figure III-6. With these characteristics only five wavelengths of the Hg source could be detected. The overall length of the array was one inch.

An 8 mW He-Ne was also used to penetrate the plume. The 0.6328  $\mu$  wavelength was used to provide a longer wavelength than that detectable by the Multispec system. A Newport photosensor diode was used with a narrow-pass He-Ne filter to eliminate ambient/plume light.

### **C. DATA ACQUISITION AND REDUCTION**

Details of the data acquisition system are presented in references 8 and 11. A Hewlett Packard HP9836S computer served as the system controller for the diode array of the white light source. Data was converted from analog to digital and stored in a HP6942A multiprogrammer. The HP9836S has two internal disk drives which were used to store data after acquisition. The program written by Harris [Ref. 11] was revised for this experiment and is presented in APPENDIX B. An electrically operated shutter was installed on the outlet of the white light source. Eight consecutive scans of the photodiode array in the exhaust were made with the shutter open, followed by four scans with the shutter closed to determine if significant radiation from the plume affected any wavelengths of the light source. An IBM PC AT computer was used to take data from the He-Ne laser. The point during the firing when the data was taken was also controlled by the IBM computer. This was accomplished by monitoring the motor chamber pressure and specifying a time delay after steady state operation was obtained.

The data was reduced in accordance with the revised computer program of Rosa [Ref. 8]. The multiple photodiode scans were averaged and the resultant scan was plotted

on a graph of voltage versus photodiode number. The digital data was also recorded. The experimentally obtained log-transmittance ratios were compared to the theoretically generated extinction-coefficient ratios from the Cashdollar program. The computer program provided the extinction coefficients vs.  $d_{32}$  as a function of standard deviation ( $\sigma$ ) and refractive index ( $m$ ) for each wavelength. The computations were repeated for different values of  $\sigma$ , refractive index ( $m$ ) and  $d_{32}$  interactively at the computer terminal until the theoretical data and experimental data coincided. Estimates for the initial values of the standard deviation ( $\sigma$ ) and the refractive of index ( $m$ ) were chosen from the literature.

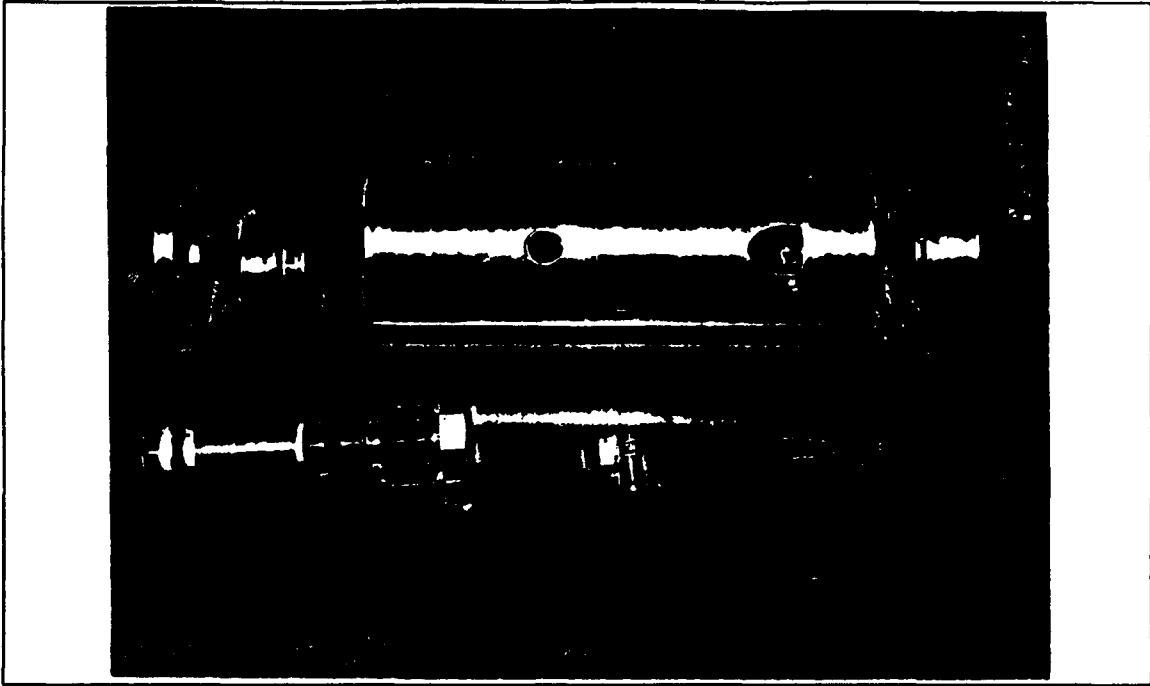


**Figure III-1. Photograph of the Motor Components**

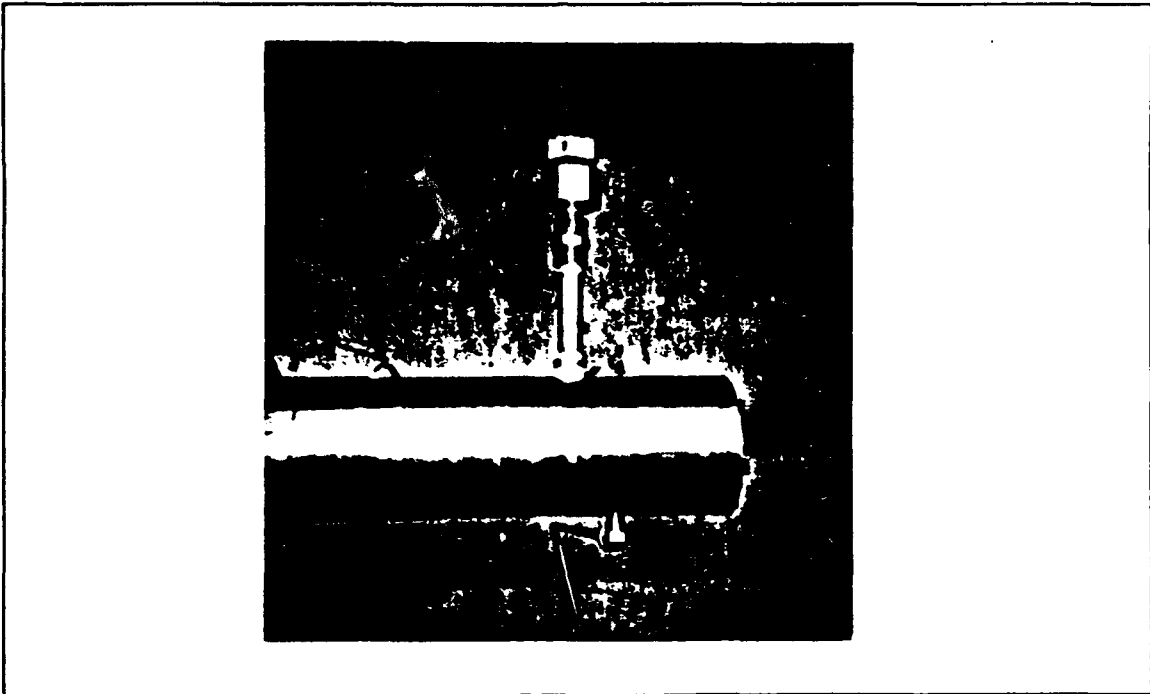


**Figure III-2. Photograph of Installed Rocket Motor**



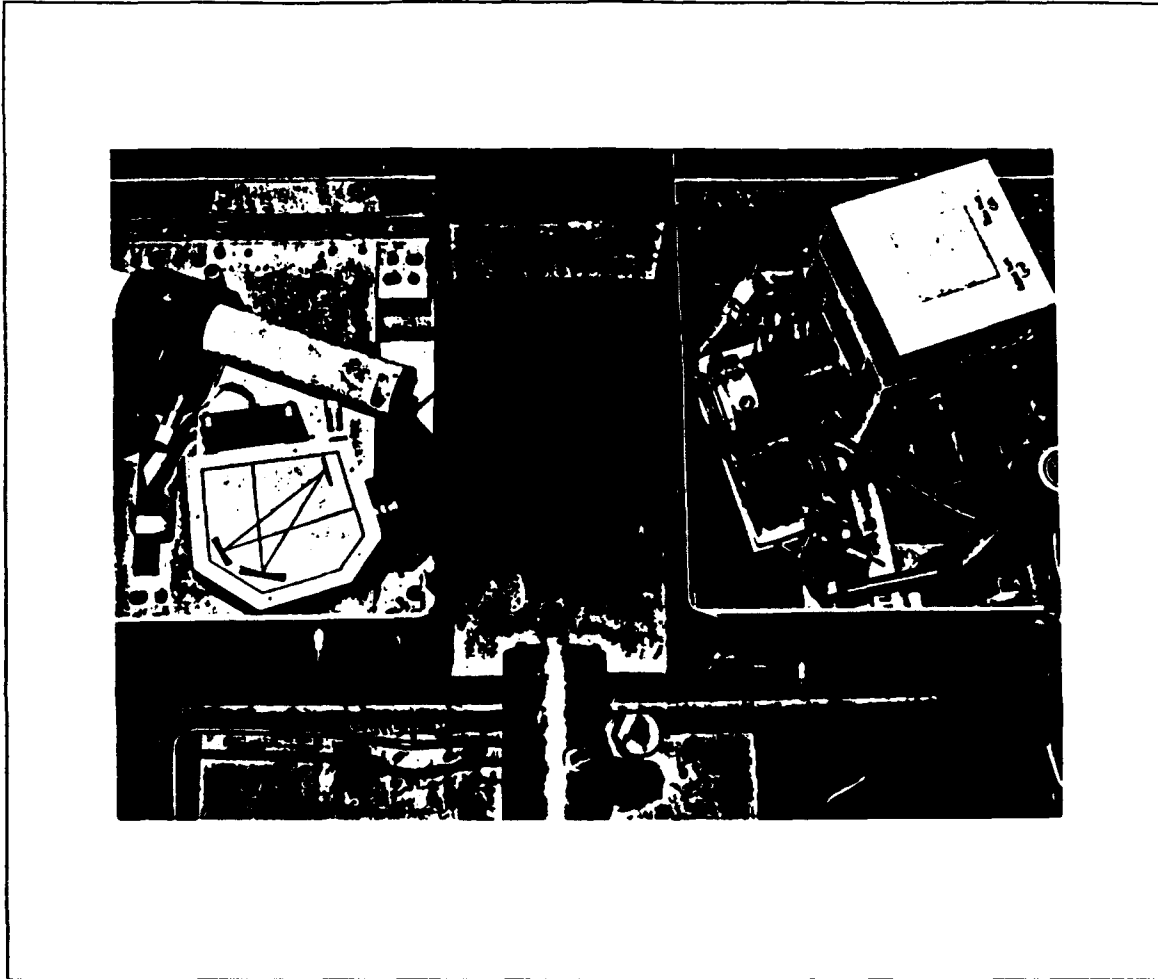


**Figure III-3. Photograph of Light Transmittance System**

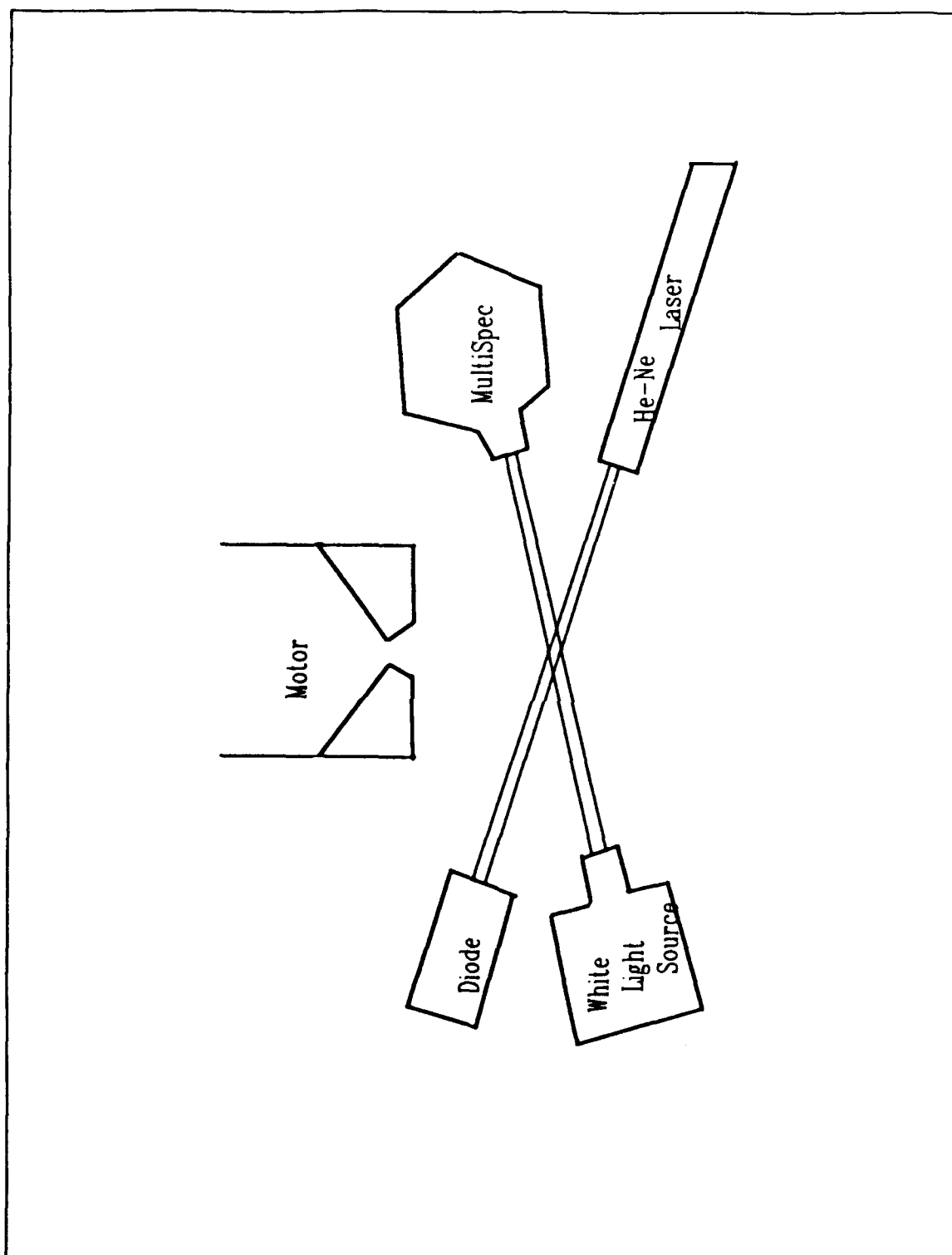


Figure III-4. Schematic Diagram of Light Transmittance Apparatus

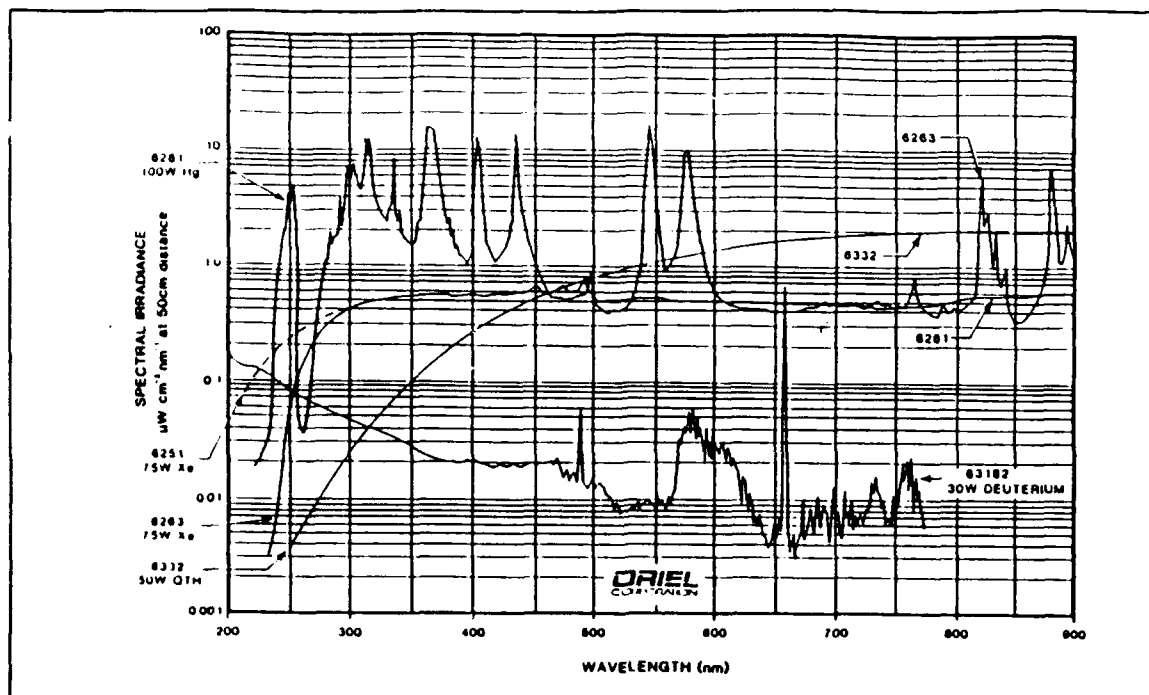


Figure III-5. Spectral Irradiance of the Hg Lamp [Ref. 9]

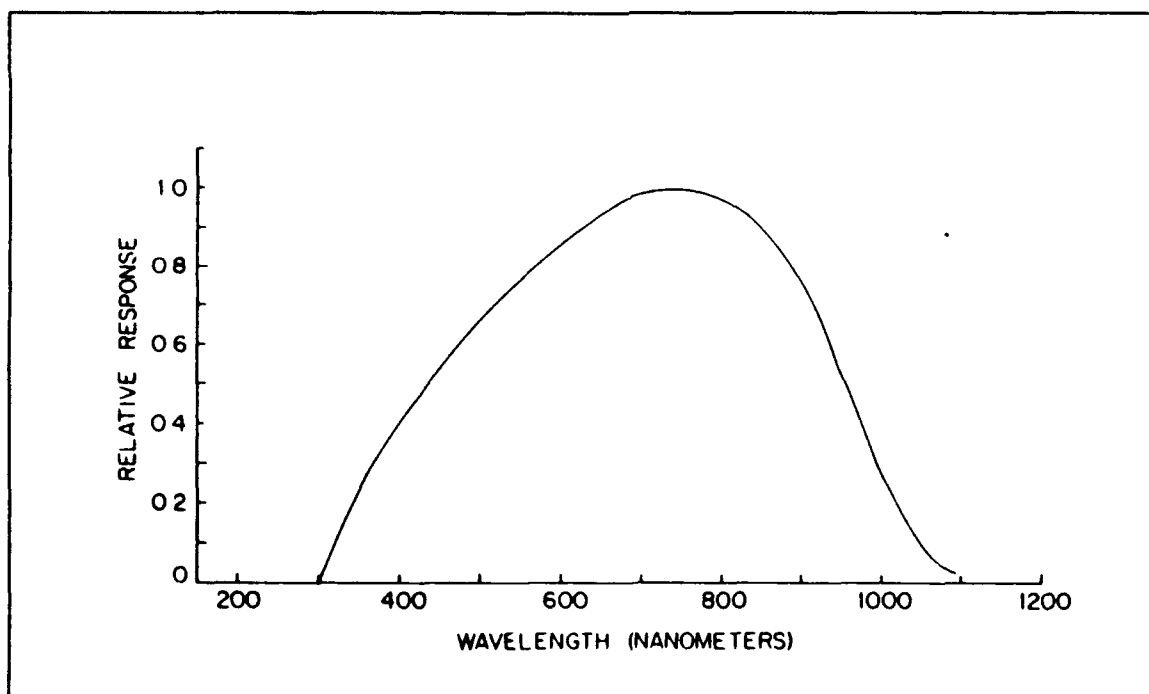


Figure III-6. Diode Spectral Response [Ref. 10]

## IV. RESULTS AND DISCUSSION

### A. INTRODUCTION

The purpose of this investigation was to measure the Sauter mean diameter ( $d_{32}$ ) and to determine the refractive index ( $m$ ) and the standard deviation ( $\sigma$ ) of an assumed log-normal size distribution of particles in the exhaust plume of a small solid propellant rocket motor. The exhaust plume can contain a broad range of particle sizes, ranging from  $0.01 \mu$  to greater than  $15 \mu$ . However, most of the particles are thought to be smaller than  $1 \mu$  in diameter. Mie theory [Ref. 6] was used to find the extinction coefficients as a function of  $d_{32}$ ,  $\lambda$ ,  $m$  and  $\sigma$ . A mercury light source was used to provide multiple wavelengths for transmission measurements. Although the mercury lamp emits ten distinct wavelength peaks, only five were measured due to the diode insensitivity to the UV (See Figures III-5 and III-6). Ten independent transmittance ratios could be obtained from these five wavelength measurements. Initially, a He-Ne IR ( $\lambda=1.525$ ) laser was also used in an attempt to provide a wider range of log-transmission ratios. However, the particles were small enough to result in transmittances of nearly 100%. Measurement uncertainty prevented use of this data. On the last test a He-Ne laser with  $\lambda=0.6328$  was used. Although the measured transmittance was quite high (~96%) the data correlated well with that obtained using the Hg light source. Use of the sixth wavelength resulted in 15 (vs. 10) independent log-transmittance ratios for correlation with the extinction coefficient ratios. Because the extinction coefficient ratios become

insensitive to  $d_{32}$  for  $d_{32}$  greater than approximately  $1\ \mu$ , the measurements had to be made in the edges of the plume where the larger particles are not thought to be present.

## **B. SYSTEM CALIBRATION**

The computer program written by Harris [Ref. 11] for recording, reducing and plotting the data from the linear diode arrays was modified for this investigation. In this investigation measurements were first made of the intensities with no particles present. During the motor firing the transmittances were measured twice, once with the light sources on and once with them off. The latter measurement was made to determine if significant radiation was emitted from the plume at the wavelengths of the light sources.

The diode array was first aligned so that the five distinct peaks of the mercury light source were correctly positioned. To determine if the system was operating correctly, it was checked using a neutral density filter with a 30% obscuration. A measurement was first made to provide the intensities of the illumination source as a function of wavelength. A second measurement was then made with the neutral density filter inserted between the light source and the diode array. The transmittance at each wavelength was then calculated by dividing the second measurement by the first. The results showed that the diode array and data acquisition system worked correctly.

## **C. ROCKET MOTOR PLUME DATA**

Seven experiments were conducted and a summary of the motor firings is tabulated in TABLE IV-1. Due to system failures, no data were obtained in four of these tests.

TABLE IV-1. SUMMARY OF MOTOR FIRINGS

Test No	Max Press	Location of Hg Light beam	Remarks
1	—	6" from Nozzle 1.0" above center	Data Trigger - failure
2	370 psig	"	1st Data
3	—	"	Data Trigger - failure
4	385 psig	"	2nd Data
5	—	13" from Nozzle center of plume	HP Computer - failure
6	410 psig	"	Contaminated - Windows
7	330 psig	7.25" from Nozzle 1.0" above center	3rd Data

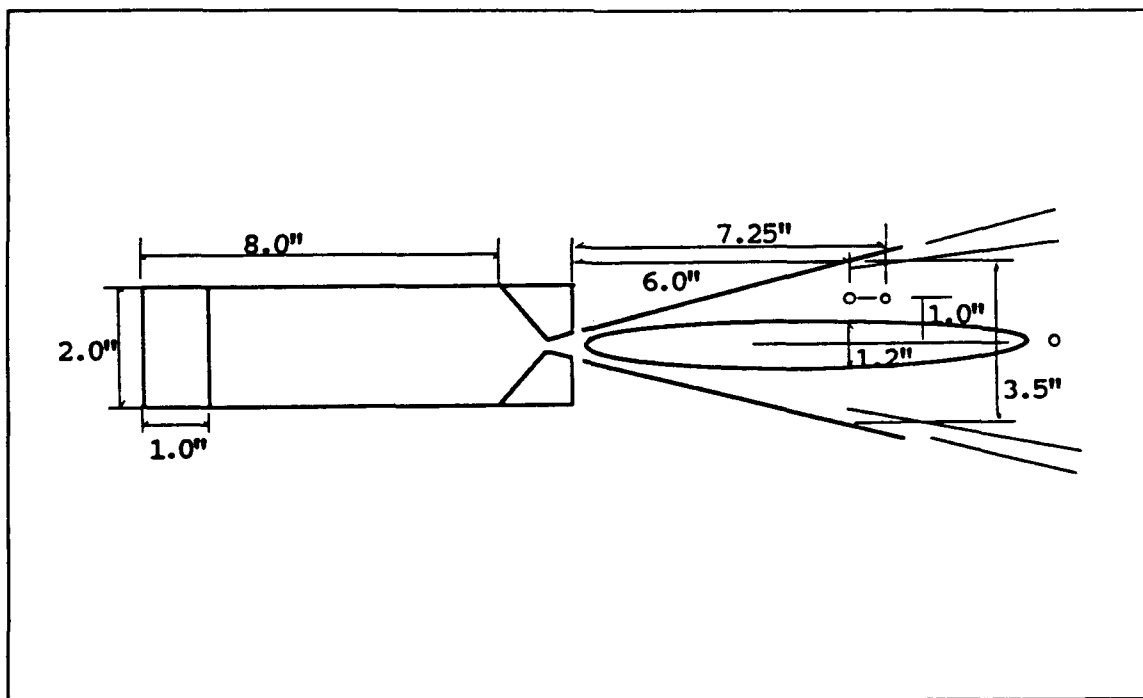


FIGURE IV-1. Configurations of the Motor and Plume

The exhaust plume was initially video recorded from above with a scaled plate positioned beneath the plume to determine the ideal positioning for the measurements. A sketch of the motor and plume is shown in Figure IV-1. An IR camera used in a related investigation also located the afterburning region within the exhaust plume. It was desired to make the transmission measurements in the outer regions of the plume to reduce the possibility of having large particles present and not to be within the afterburning region where high plume radiation is present. However, it was necessary to be close enough to the exhaust nozzle as possible to provide as steady a plume flowfield as possible. The measurement locations are shown Figure IV-1, 16-19 nozzle exit diameters (6-7.25") downstream and 5.25 nozzle exit radii (1.0") from the plume centerline.

The "lights-on"/"lights-off" measurements during the motor firings indicated that no significant plume radiation was present at the measurement location for the wavelengths of the illumination sources. Each run, therefore, provided two sets of data; one for 100% transmittance (before the firing) and the other with the plume particles present. Eight scans of the diode array were taken in 0.24 seconds. Any obviously bad scans were eliminated and the remaining scan voltages were averaged. The analog results are shown in Figures IV-2 through IV-7. The digital data was also recorded and is presented in APPENDIX A. Peak voltages on the array for each wavelength generally occurred over several diodes. During a motor firing some steering of the illuminating beam also occurs due to density gradients in the plume. The unsteadiness of the plume also resulted in some fluctuations in both the peak voltages and the diodes on which the peaks occurred.

TABLE IV-2. DIODE READINGS AND TRANSMITTANCE

	Wavelength,	$\lambda=.365$	$\lambda=.4047$	$\lambda=.4358$	$\lambda=.5461$	$\lambda=.577$
1	W/O Plume	217-221 (.00520)	341-346 (.00542)	436-448 (.00531)	789-798 (.00625)	888-897 (.00645)
	With Plume	213-222 (.00460)	339-346 (.00494)	436-446 (.00491)	787-799 (.00600)	890-901 (.00622)
	Transmittance	88.46 %	91.15 %	92.49 %	96.0 %	96.46 %
2	W/O Plume	219-227 (.00481)	344-348 (.00468)	439-446 (.00554)	787-802 (.00608)	887-901 (.00559)
	With Plume	220-228 (.00430)	345-348 (.00430)	438-443 (.00515)	789-799 (.00588)	889-898 (.00543)
	Transmittance	89.37 %	91.88 %	93.0 %	96.72 %	97.08 %
3	W/O Plume	214-224 (.00568)	340-343 (.00475)	434-444 (.00568)	784-799 (.00616)	885-899 (.00563)
	With Plume	217-223 (.00460)	340-344 (.00400)	438-444 (.00491)	789-800 (.00575)	888-903 (.00532)
	Transmittance	80.96 %	84.21 %	86.52 %	93.4 %	94.42 %

TABLE IV-3. LOG TRANSMISSION RATIOS

	1st run	2nd run	3rd run
$\lambda_{.5770}/\lambda_{.3650}$	0.294	0.264	0.272
$\lambda_{.5461}/\lambda_{.3650}$	0.333	0.297	0.323
$\lambda_{.5770}/\lambda_{.4047}$	0.389	0.350	0.334
$\lambda_{.5461}/\lambda_{.4047}$	0.441	0.394	0.397
$\lambda_{.5770}/\lambda_{.4358}$	0.462	0.408	0.396
$\lambda_{.5461}/\lambda_{.4358}$	0.523	0.460	0.471
$\lambda_{.4358}/\lambda_{.3650}$	0.637	0.646	0.686
$\lambda_{.4047}/\lambda_{.3650}$	0.756	0.754	0.814
$\lambda_{.4358}/\lambda_{.4047}$	0.843	0.857	0.843
$\lambda_{.5770}/\lambda_{.5461}$	0.883	0.889	0.841



In general, peak voltages were present on several diodes and then dropped off rapidly on either side. These peak voltages were then averaged. The diode numbers for each peak, the average voltages and the calculated transmittances are presented in TABLE IV-2. TABLE IV-3 presents the log-transmittance ratios.

Assuming the refractive index (with absorption index = 0) of the plume particles was independent of wavelength, extinction coefficients were calculated for each wavelength using the Mie code [Ref. 5] and are shown in Figure IV-8. Extinction coefficient ratios were then calculated as shown in Figure IV-9. The unknowns to be determined were  $m$ ,  $\sigma$  and  $d_{32}$ . This was accomplished in an iterative manner, starting with expected values taken from the literature. The iteration scheme is shown in Figure IV-10. In order to determine the best fit with the experimental data, a regression analysis method [Ref. 12] was used. The log-transmittance ratios were plotted against the extinction coefficient ratios. A linear least-squares fit of the data was then made; a perfect fit having a slope of unity and an  $R^2$  of unity.  $R^2$  is defined by

$$R^2 = \frac{\sum (y_{est} - \bar{y})^2}{\sum (y - \bar{y})^2} = \frac{\text{Explained-variation}}{\text{Total-variation}}$$

" $R^2$  can be interpreted as the fraction of the total variation which is explained by the least-squares regression line. If the total variation is all explained by the regression line, i.e. if  $R^2 = 1$ , we say that there is perfect linear correlation (and in such case also perfect linear regression). On the other hand if the total variation is all unexplained then the explained variation is zero and so  $R=0$ . In practice the quantity  $R^2$ , sometimes called

TABLE IV-4 . REGRESSION ANALYSIS FOR THE RUNS

		1st plume	2nd plume	3rd plume	Remarks
1	X-Coefficient(slope) Err from Slope R squared	0.8589 0.0289 0.9455	0.8841 0.0176 0.9809	0.8759 0.0229 0.9671	$d_{32} = .09$ $\sigma = 1.5$ $m = 1.7-0i$
2	X-Coefficient(slope) Err from Slope R squared	0.9263 0.0172 0.9790	0.9512 0.0118 0.9905	0.9434 0.0131 0.9883	$d_{32} = .12$ $\sigma = 1.5$ $m = 1.7-0i$
3	X-Coefficient(slope) Err from Slope R squared	0.9991 0.0129 0.9868	1.0235 0.0231 0.9599	1.0162 0.0186 0.9736	$d_{32} = .15$ $\sigma = 1.5$ $m = 1.7-0i$
4	X-Coefficient(slope) Err from Slope R squared	0.9061 0.0203 0.9716	0.9310 0.0117 0.9910	0.9231 0.0154 0.9841	$d_{32} = .15$ $\sigma = 1.3$ $m = 1.7-0i$
5	X-Coefficient(slope) Err from slope R squared	1.0628 0.0219 0.9553	1.0860 0.0395 0.8622	1.0785 0.0357 0.8855	$d_{32} = .15$ $\sigma = 1.7$ $m = 1.7-0i$
6	X-Coefficient(slope) Err from Slope R squared	0.9959 0.0102 0.9916	1.0199 0.0229 0.9596	1.0121 0.0208 0.9662	$d_{32} = .12$ $\sigma = 1.7$ $m = 1.7-0i$
7	X-Coefficient(slope) Err from Slope R squared	0.9663 0.0092 0.9935	0.9904 0.0169 0.9790	0.9824 0.0176 0.9769	$d_{32} = .15$ $\sigma = 1.5$ $m = 1.5-0i$
8	X-Coefficient(slope) Err from Slope R squared	1.0174 0.0155 0.9805	1.0417 0.0271 0.9433	1.0346 0.0214 0.9641	$d_{32} = .15$ $\sigma = 1.5$ $m = 1.9-0i$
9	X-Coefficient(slope) Err from Slope R squared	0.9736 0.0816 0.9948	0.9976 0.0186 0.9744	0.9895 0.0191 0.9723	$d_{32} = .12$ $\sigma = 1.7$ $m = 1.5-0i$
10	X-Coefficient(slope) Err from Slope R squared	1.0266 0.0146 0.9818	1.0505 0.0296 0.9294	1.0429 0.0259 0.9451	$d_{32} = .12$ $\sigma = 1.7$ $m = 1.9-0i$
11	X-Coefficient(slope) Err from Slope R squared	0.9771 0.0100 0.9925	1.0000 0.0182 0.9763	0.9931 0.0170 0.9782	$d_{32} = .15$ $\sigma = 1.5$ $m = 1.63-0i$

the coefficient of determination, lies between 0 and 1" [Ref 13]. The particle refractiveindex was varied from 1.5 to 1.9 and  $\sigma$  from 1.3 to 1.7 (see TABLE IV-4 for representative results). This iteration process was accomplished using the ten wavelength ratios provided by the mercury light source and resulted in  $d_{32}=0.15$  ,  $\sigma=1.5$  and  $m=1.63$ . The extinction coefficients and extinction coefficient ratios shown in Figures IV-8 and IV-9 were calculated using these values.

In the above process it was necessary to estimate how accurately the values of  $d_{32}$ ,  $\sigma$  and  $m$  could be determined. This was accomplished by perturbing each variable independently about the nominal values given above and observing the changes in the plotted fit to the data and the values of X-coefficient. The results are shown in Figures IV-11 through IV-13 and in TABLE IV-5. From this analysis, for 1 % variation in X-coefficient (Slope) the measured values of  $d_{32}$ ,  $\sigma$  and  $m$  were determined to be as follows:

$$d_{32} = 0.150 \pm 0.006 \mu$$

$$\sigma = 1.50 \pm 0.04$$

$$m = 1.63 \pm 0.13$$

It is seen from these results that the multiple-wavelength transmission method (for the wavelengths used and the particle sizes present) can determine  $\sigma$  and  $d_{32}$  quite accurately and without much sensitivity to  $m$ . The refractive index cannot be determined as accurately using the present system.

Using the above values for  $d_{32}$ ,  $\sigma$  and  $m$ , the data from all three motor firings are shown in Figure IV-14 for the five wavelengths of the mercury light source. The test-to test data were observed to be very repeatable. Another aspect of the technique utility is

TABLE IV-5. ESTIMATES OF MEASUREMENT ACCURACY, RUN 2

	X-Coefficient ( $R^2$ )	Estimated Accuracy ( 1 % deviation)
Sensitivity to $d_{32}$ (Fig. IV-11) = 0.144 $\mu$ = 0.150 $\mu$ = 0.155 $\mu$	0.990 (0.980) 1.000 (0.982) 1.016 (0.963)	$\pm 0.006$
Sensitivity to $\sigma$ (Fig. IV-12) = 1.47 = 1.50 = 1.54	0.990 (0.971) 1.000 (0.982) 1.012 (0.967)	$\pm 0.04$
Sensitivity to $m$ (Fig. IV-13) = 1.50 = 1.63 = 1.70	0.989 (0.979) 1.000 (0.982) 1.023 (0.959)	$\pm 0.13$

related to the accuracy of the measured transmittances. The required accuracy increases as  $\lambda$  increases and as the spread between the  $\lambda$ 's decreases. This can be seen in Figure IV-14. The accuracy of the transmittance measurements was approximately 0.5 %. The resulting uncertainty bands for  $\ln Tr(\lambda_5)/\ln Tr(\lambda_1)$  are much less than for  $\ln Tr(\lambda_5)/\ln Tr(\lambda_4)$  where the wavelengths are much more closely spaced. The difference in wavelengths between  $\lambda_5$  and  $\lambda_4$  and between  $\lambda_3$  and  $\lambda_2$  are approximately equal (.031  $\mu$ ). However, the log transmittance ratios for the lower wavelengths result in less uncertainty due to the lower values of transmittance. The data obtained in test 3 using the fifteen log-transmittance ratios provided by both the mercury and He-Ne light sources are shown in Figure IV-15. The additional ratios correlated well with the ten mercury lamp ratios and increased confidence in the data.

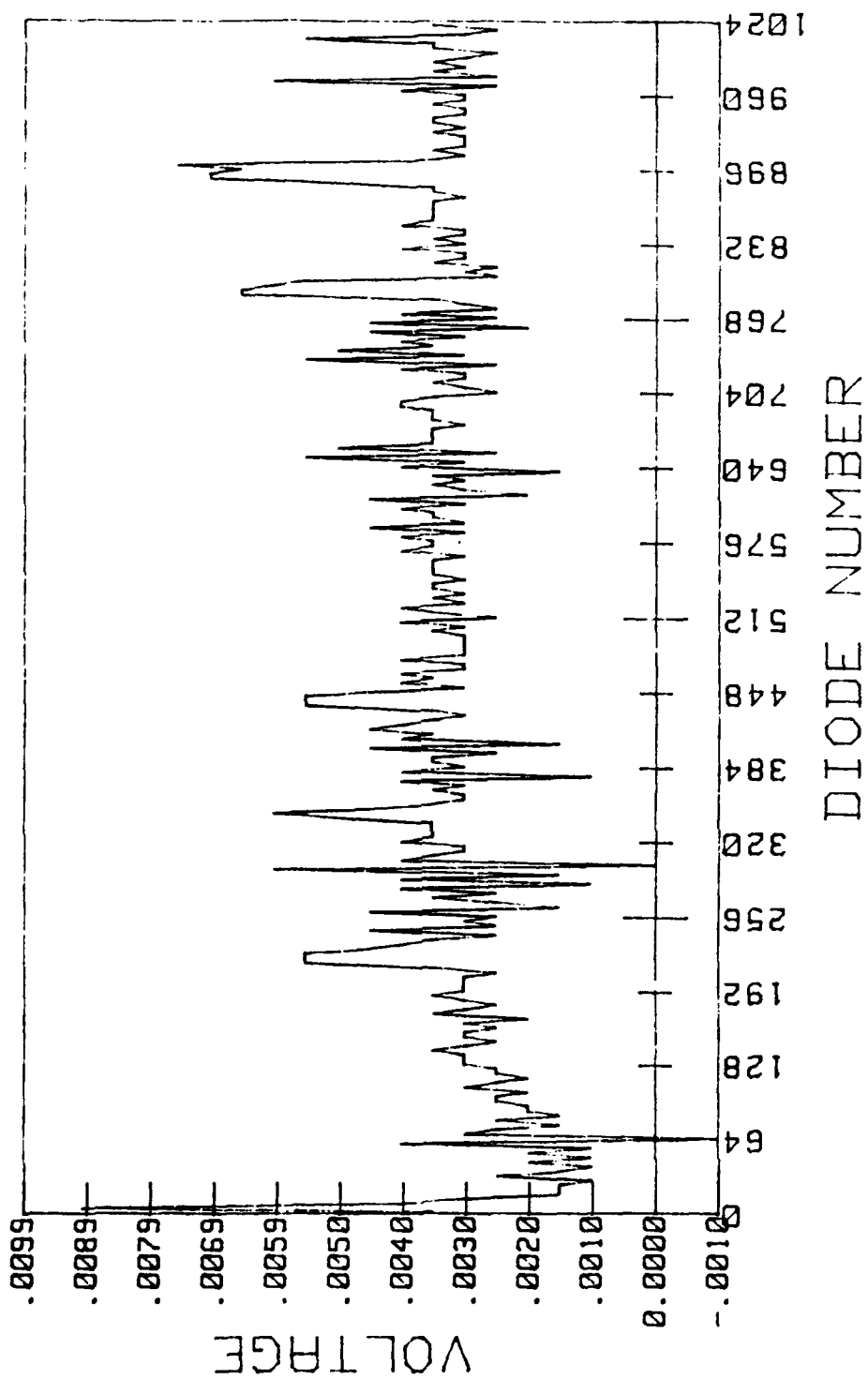


Figure IV-2. Voltage vs. Diode Number Run 1 without Plume

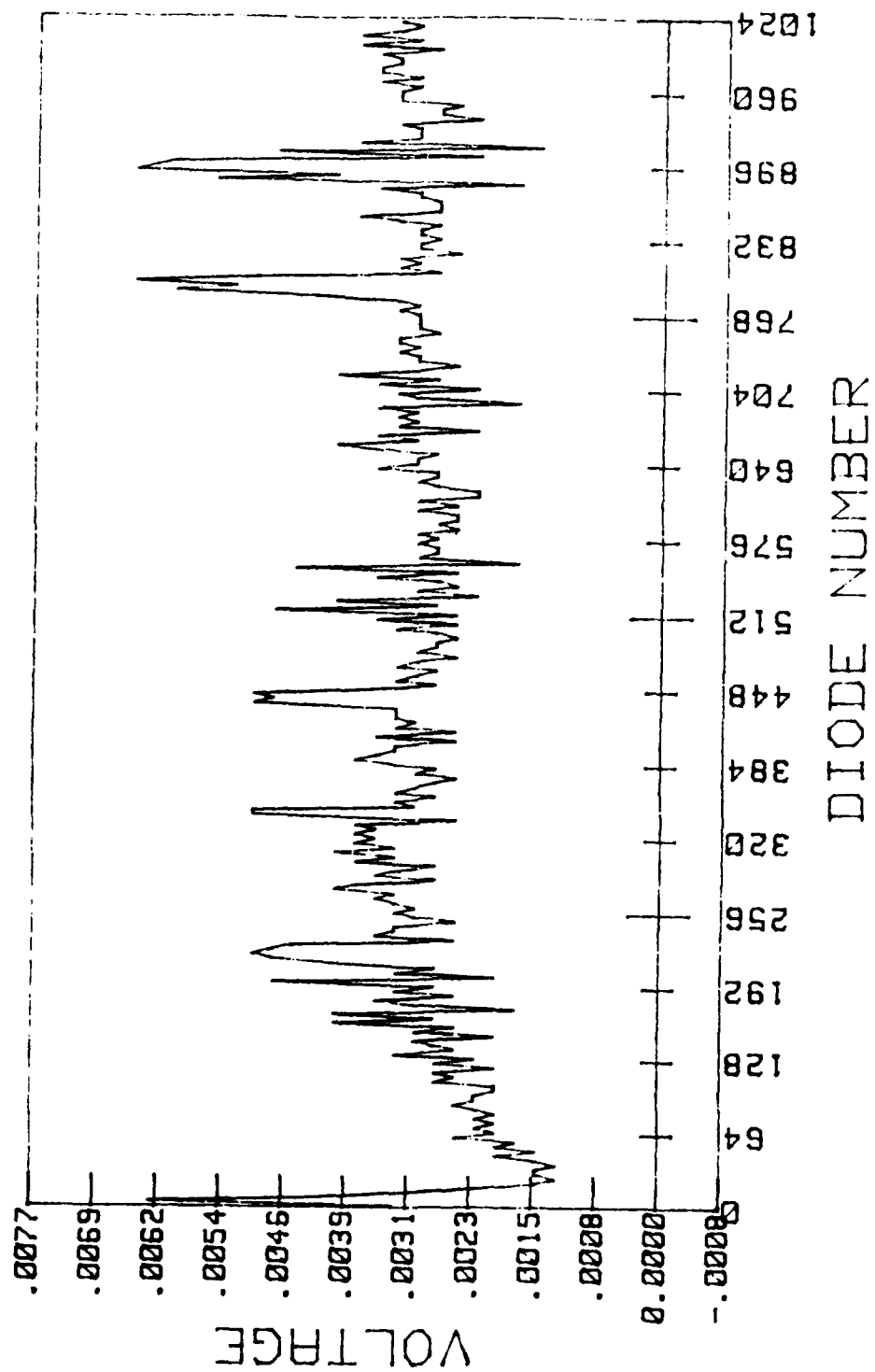


Figure IV-3. Voltage vs. Diode Number, Run 1, in Plume

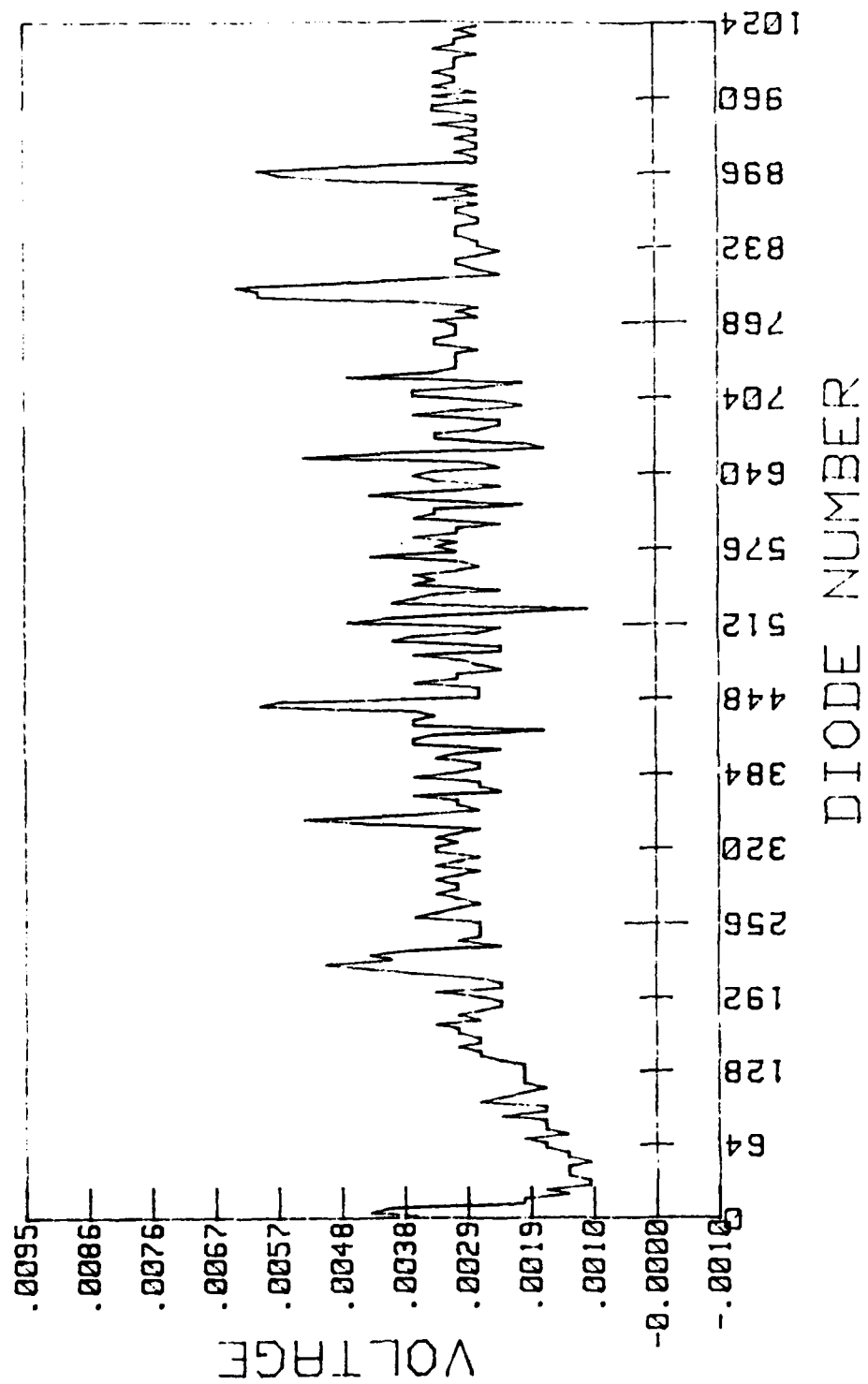


Figure IV-4. Voltage vs. Diode Number, Run 2, without Plume

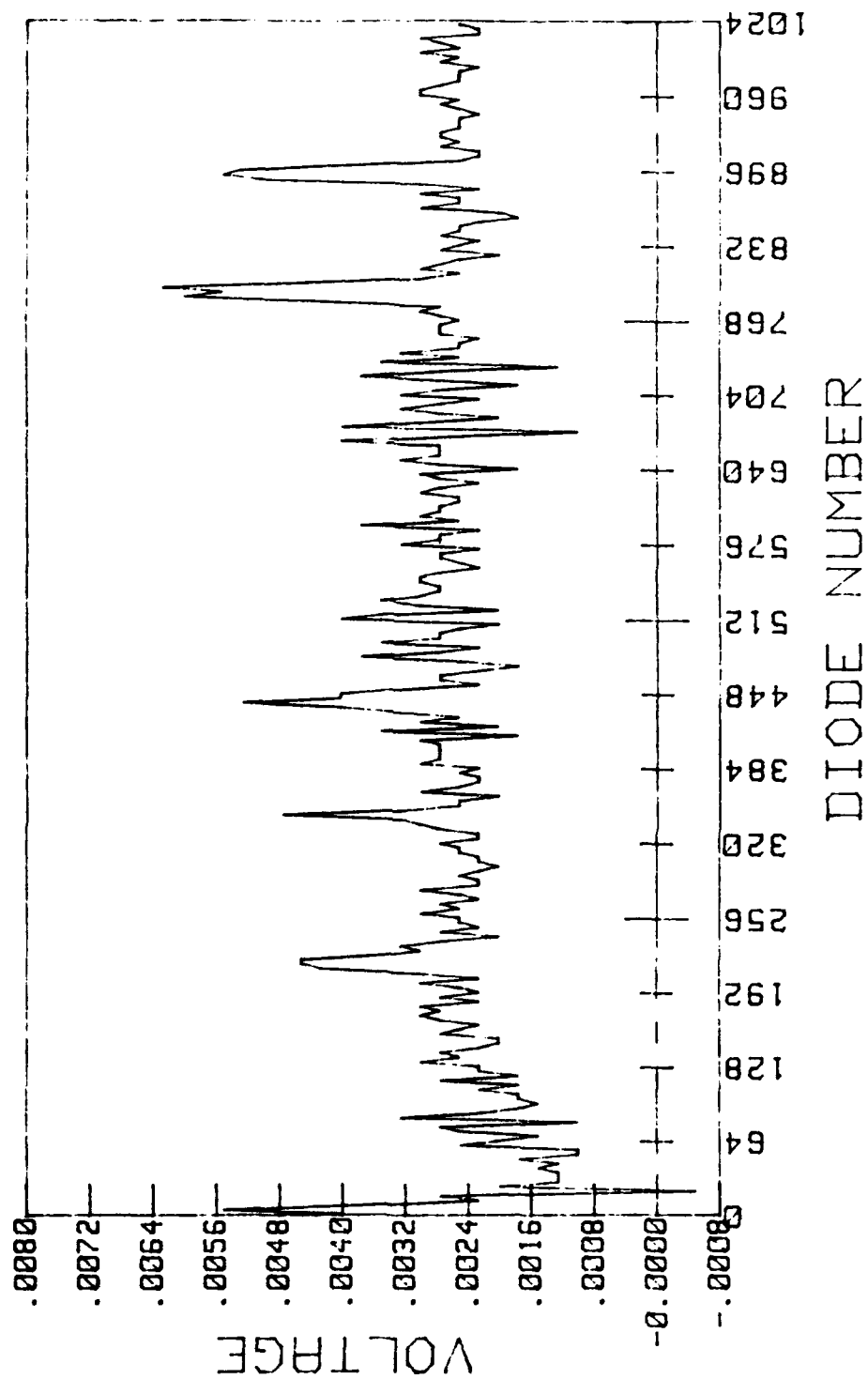


Figure IV-5. Voltage vs. Diode Number, Run 2, in Plume



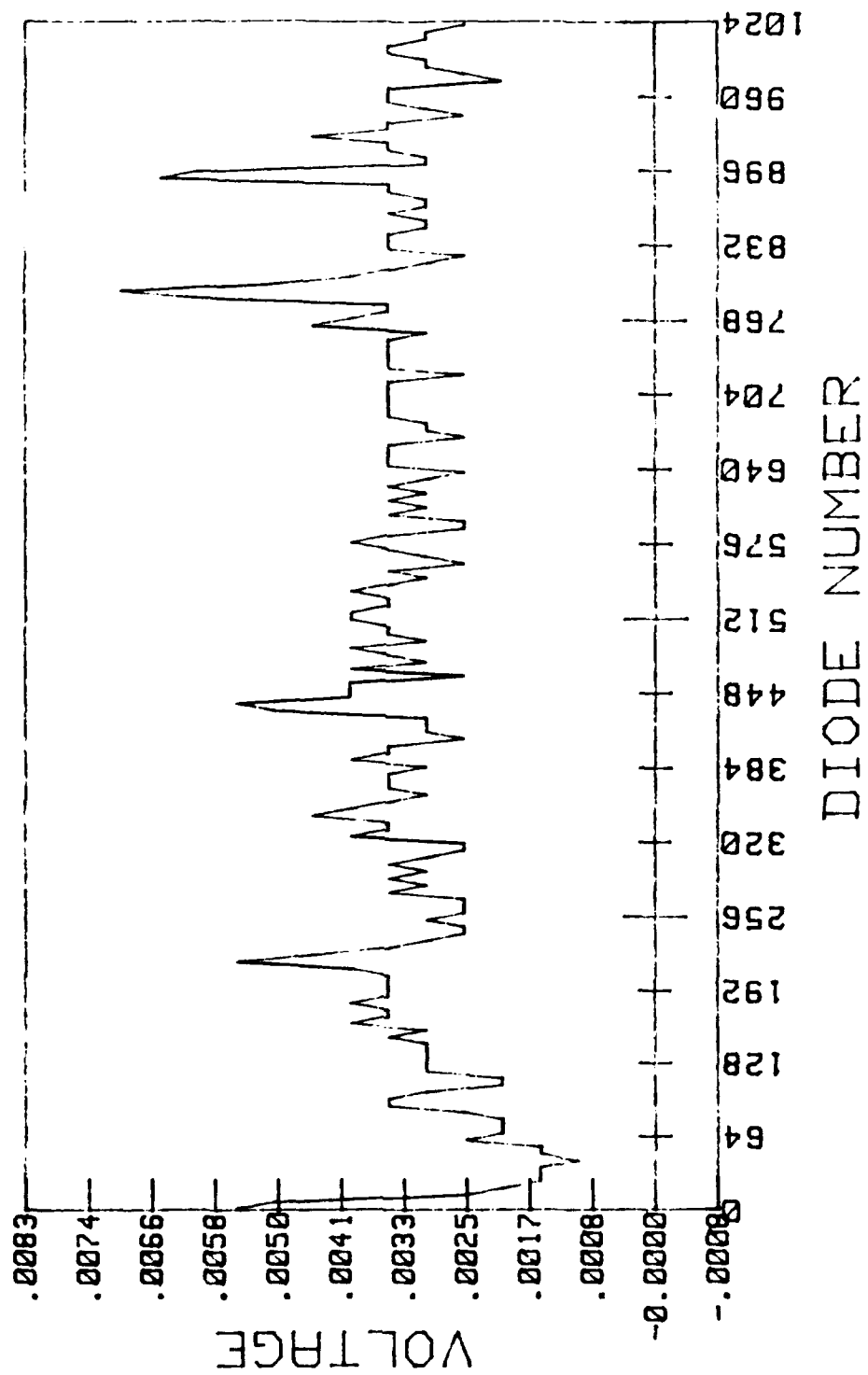


Figure IV-6. Voltage vs. Diode Number, Run 3, without Plume

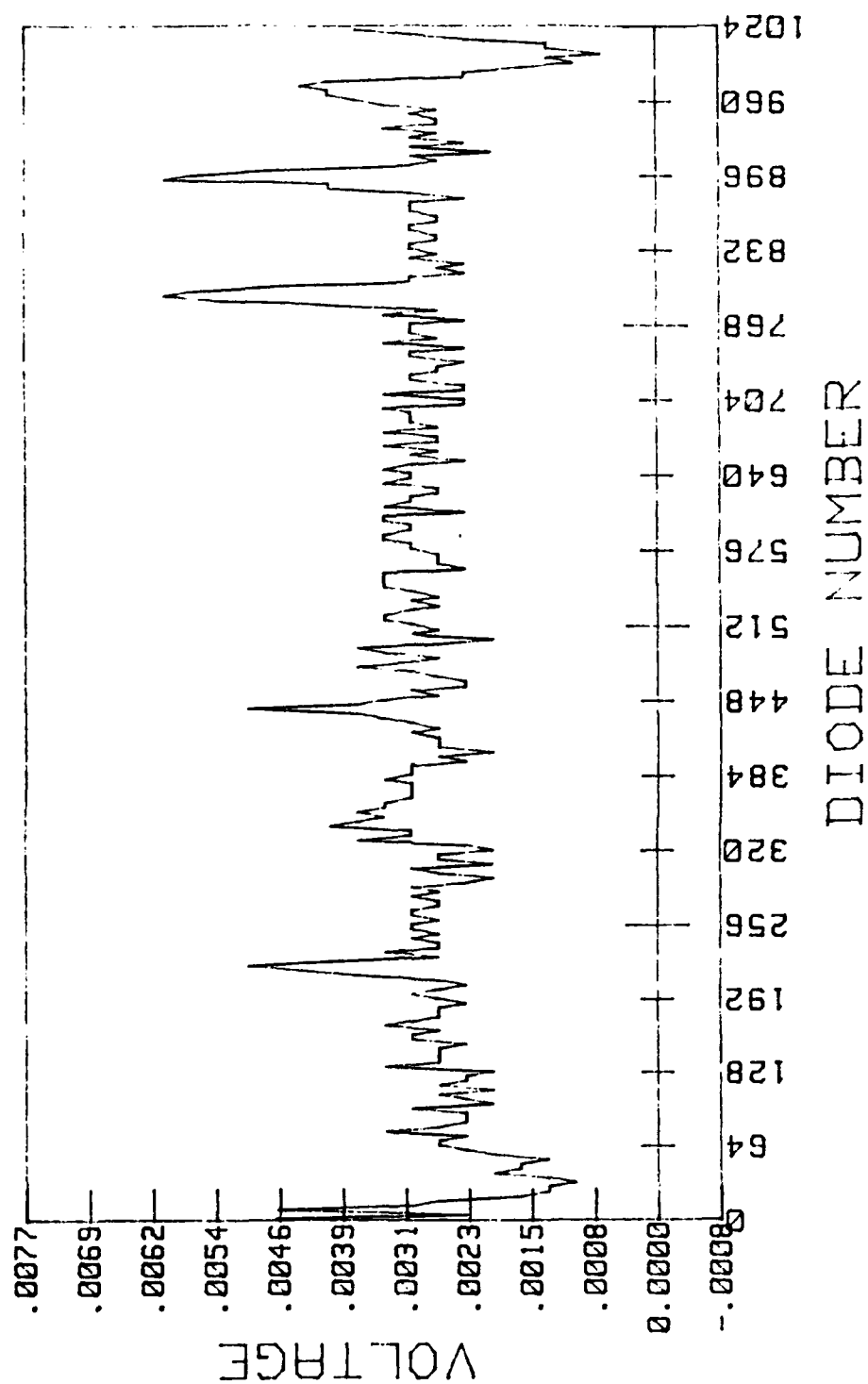


Figure IV-7. Voltage vs. Diode Number, Run 3, in Plume

# extinction coefficients

with  $\sigma = 1.5, m = 1.63 - 0i$

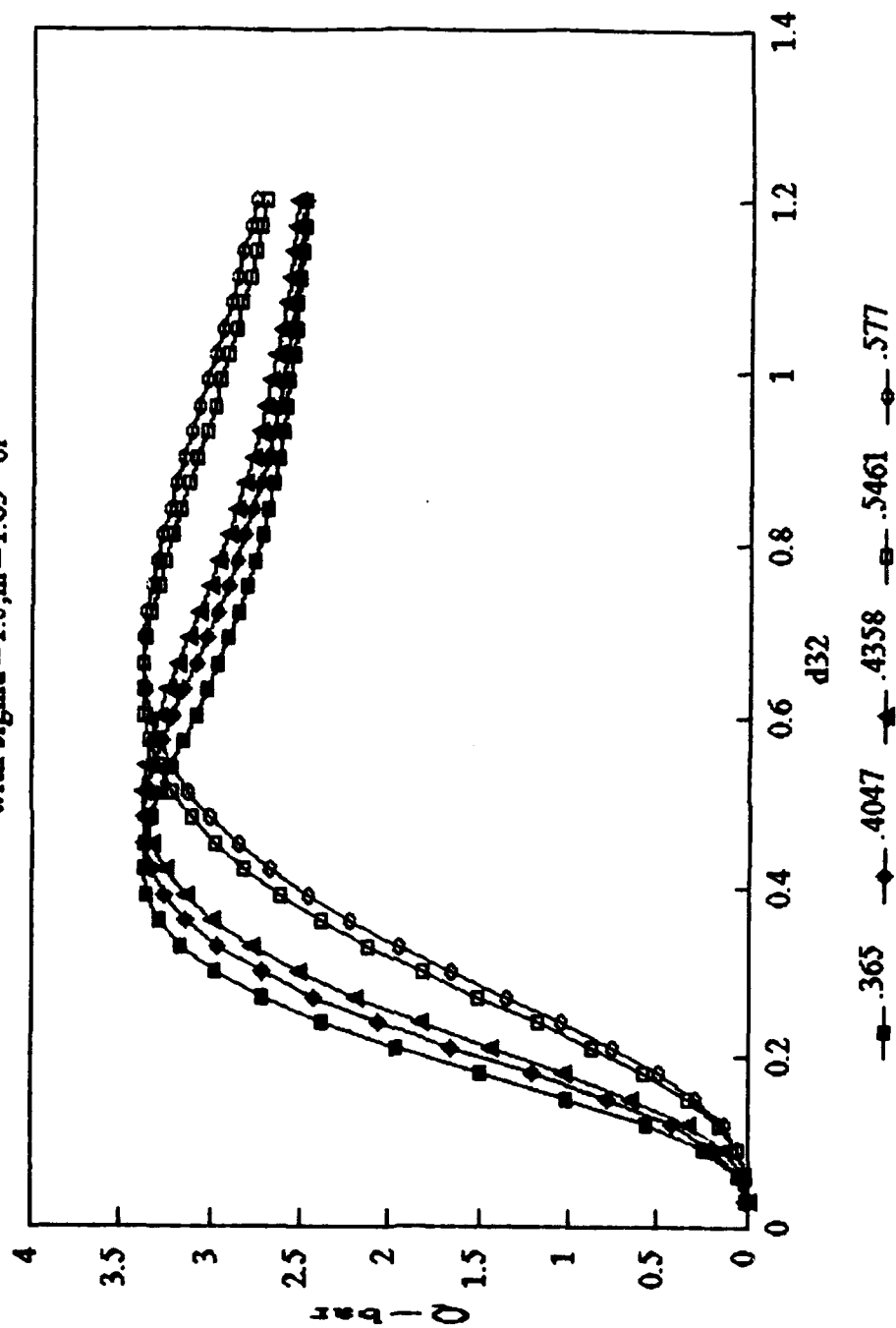


Figure IV-8. Extinction Coefficients

# extinction coefficient ratios

with  $\sigma = 1.5, m = 1.63 - 0i$

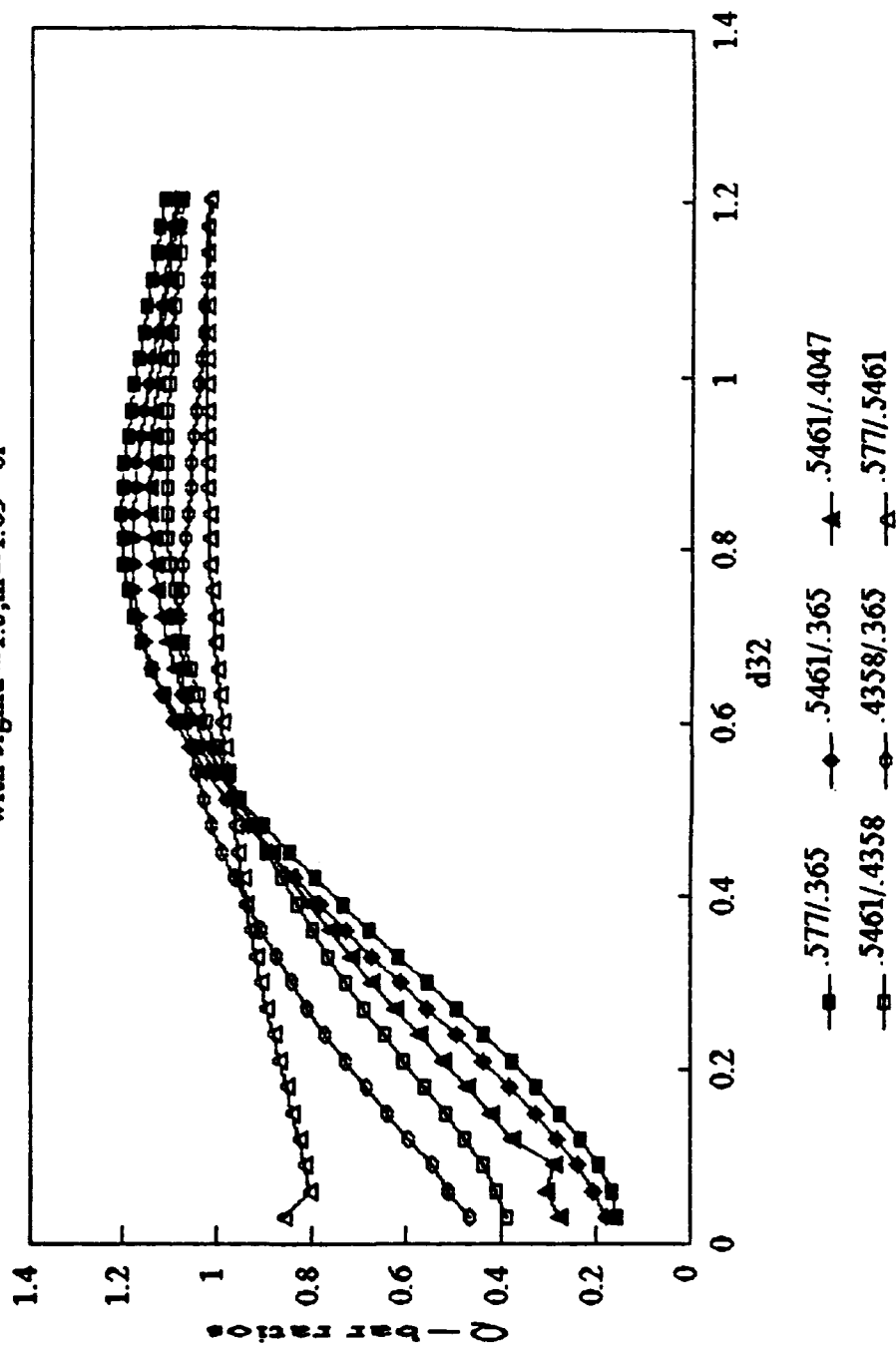


Figure IV-9. Extinction Coefficient Ratios

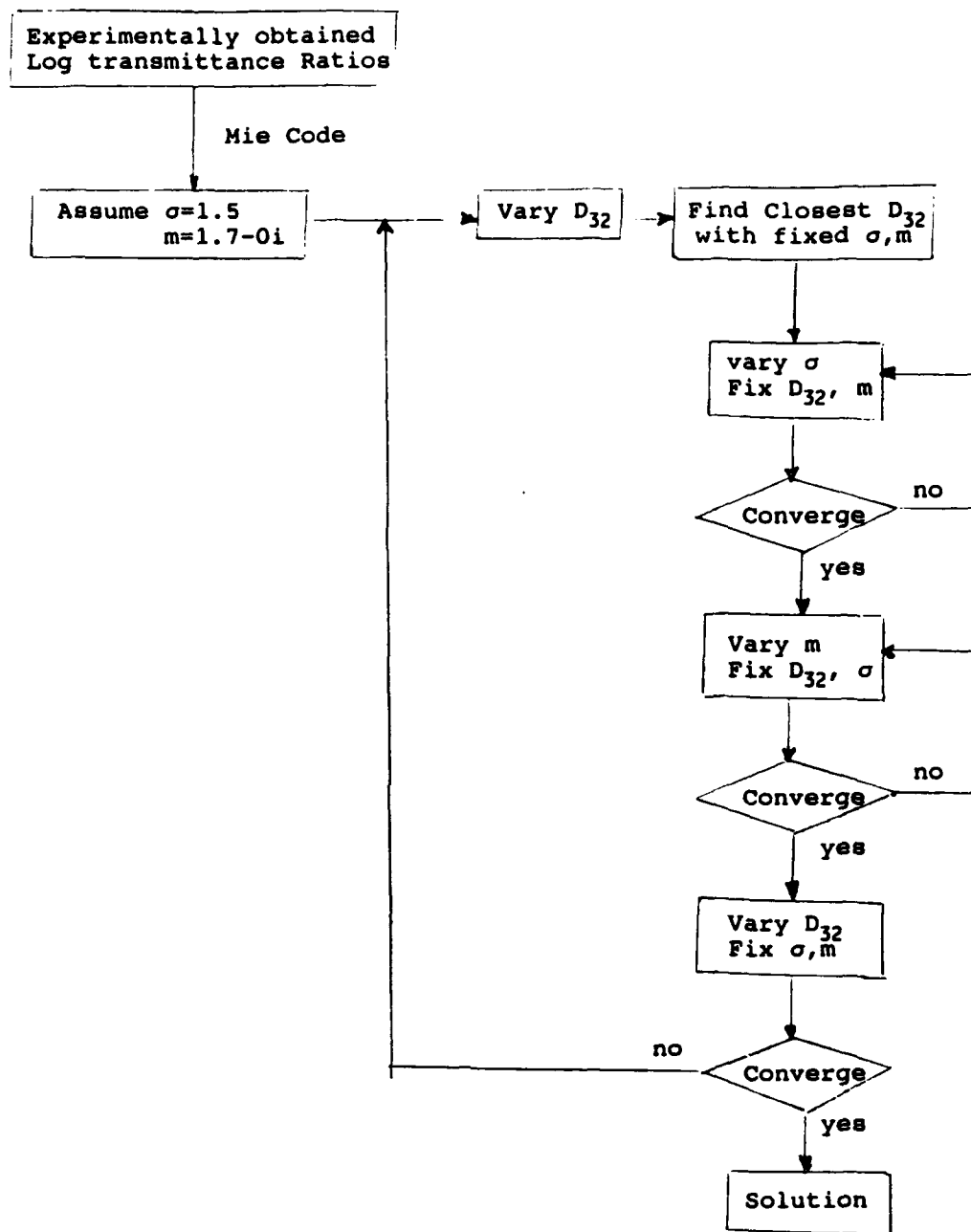


Figure IV-10. Iteration Flow Scheme

# **d32 sensitivity** with $\sigma = 1.5$ , $m = 1.63 - 0i$

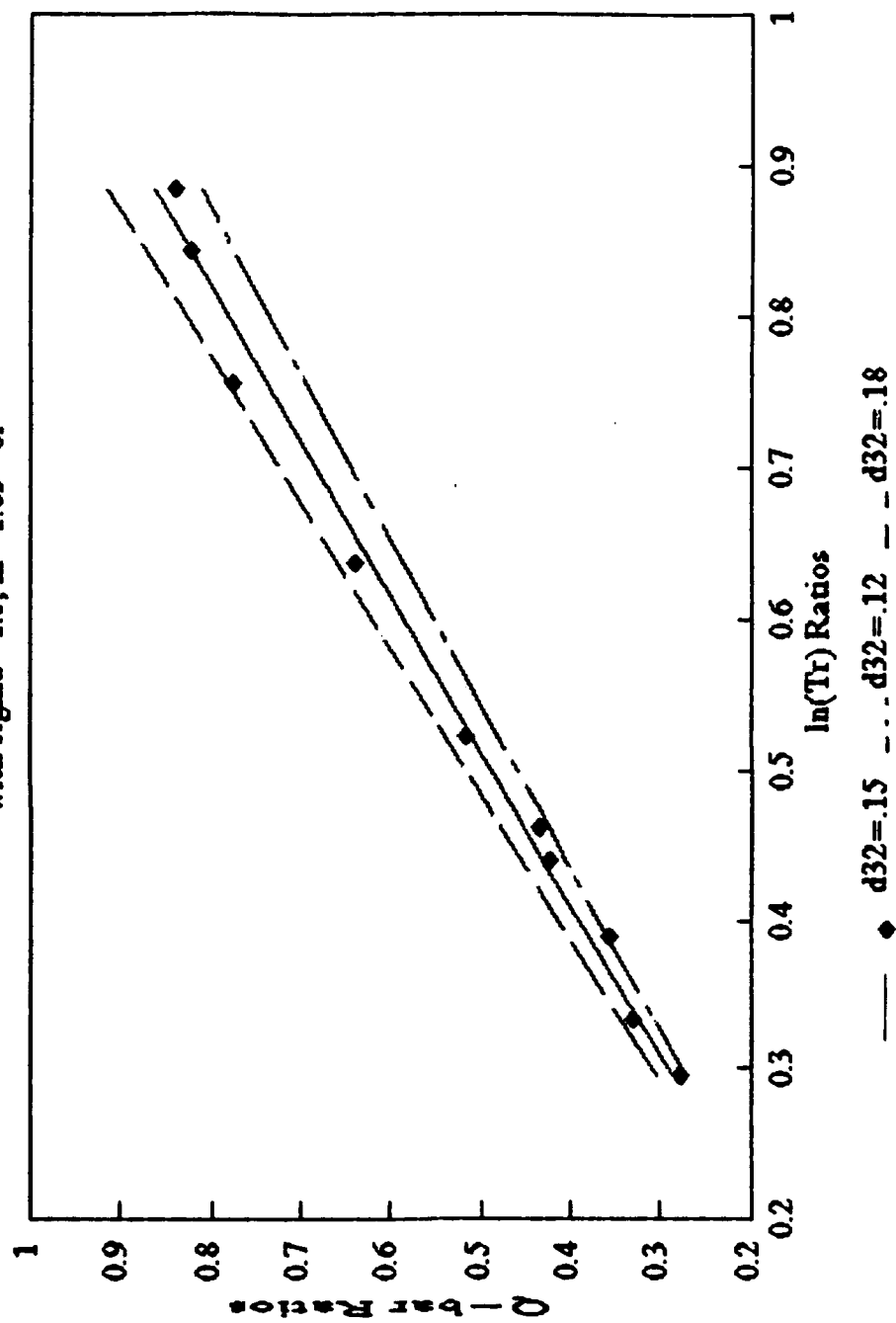


Figure IV-11. Data Correlation Sensitivity for Specified  $D_{32}$ , Run 1

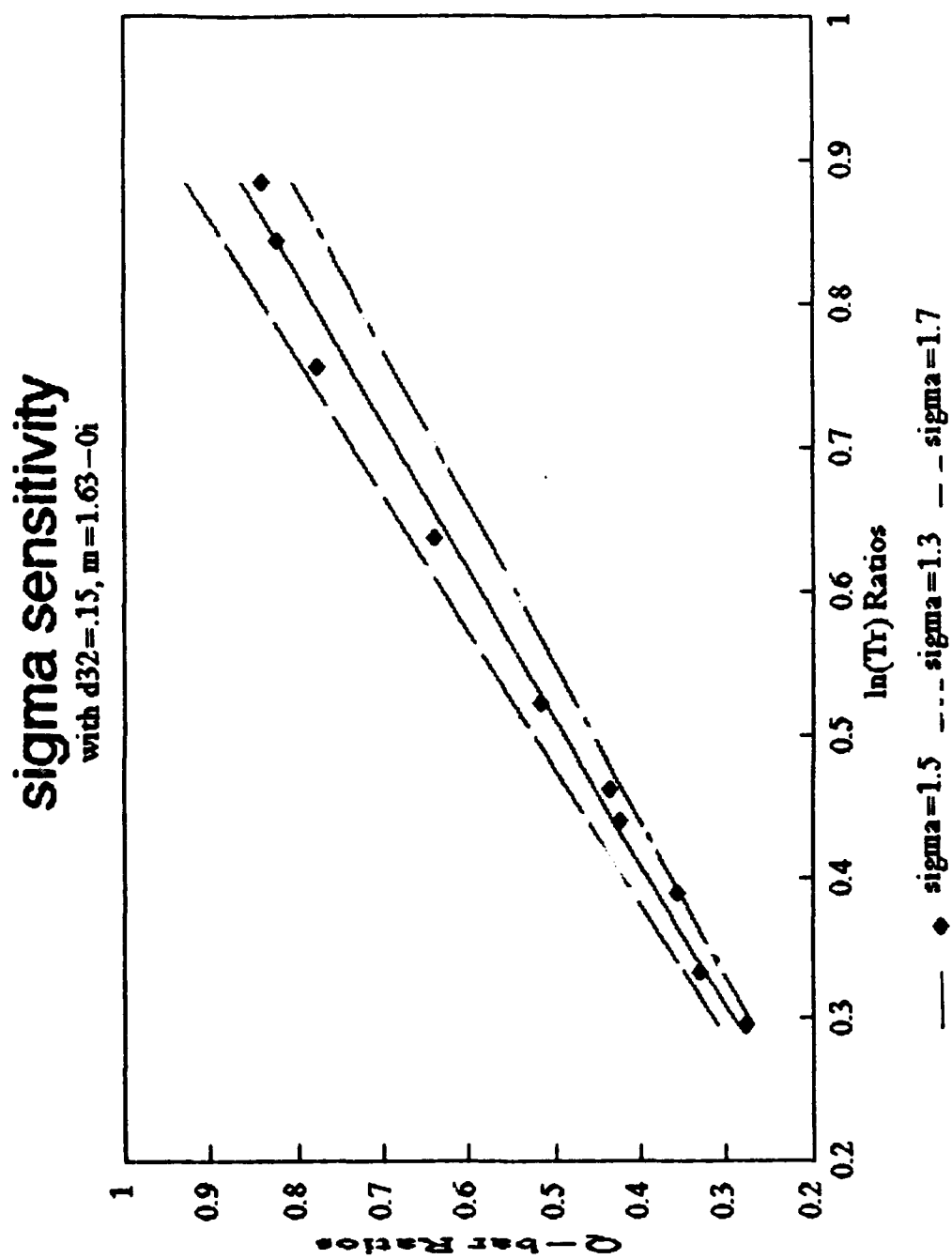


Figure IV-12. Data Correlation Sensitivity for Specified  $\sigma$ , Run 1

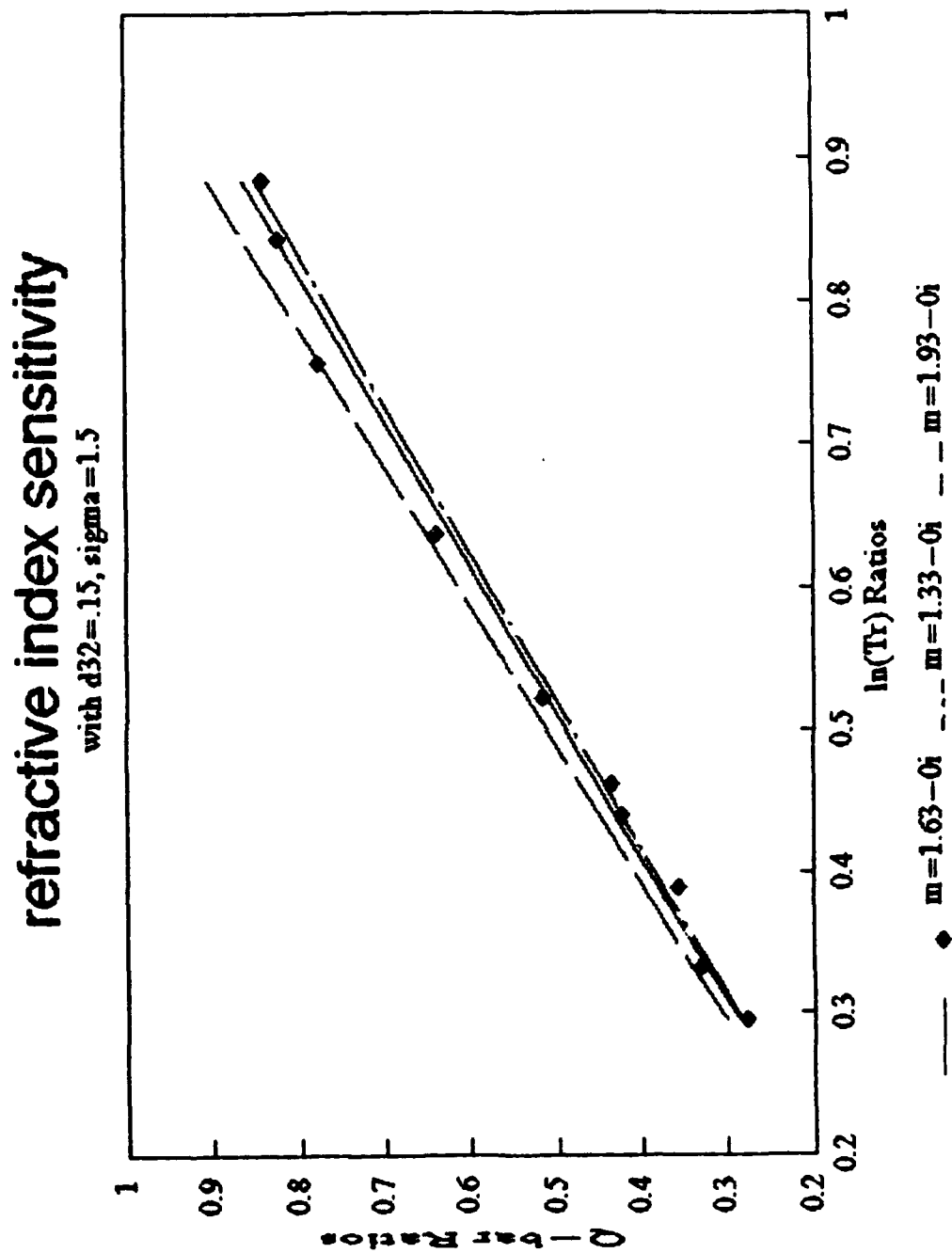


Figure IV-13. Data Correlation Sensitivity for Specified  $m$ , Run 1



data from 3--runs  
with  $d_{32}=15$ ,  $\sigma=1.5$ ,  $m=1.63-0i$

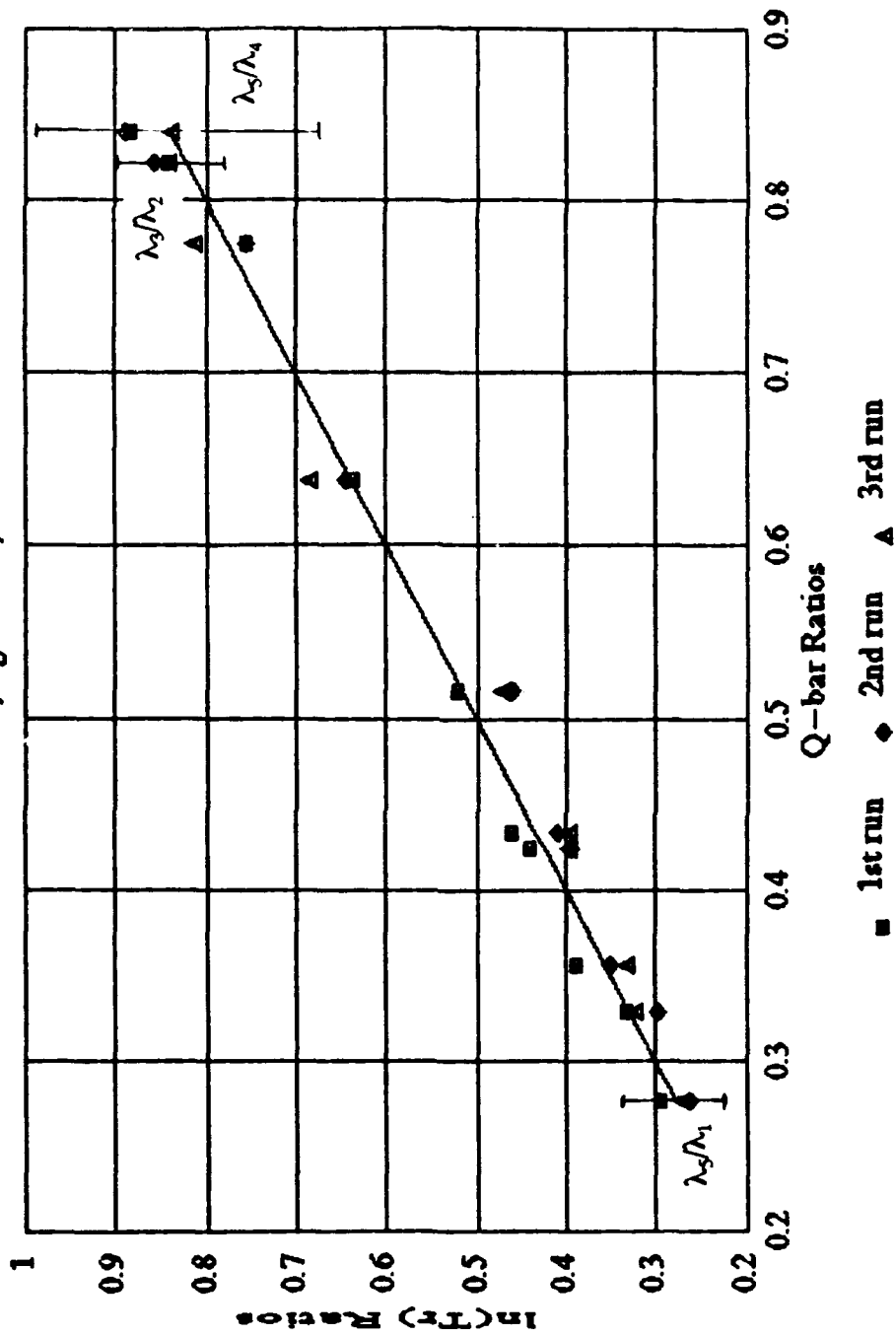


Figure IV-14. Log Transmission vs. Extinction Coefficient Ratios, Run 1,2 & 3

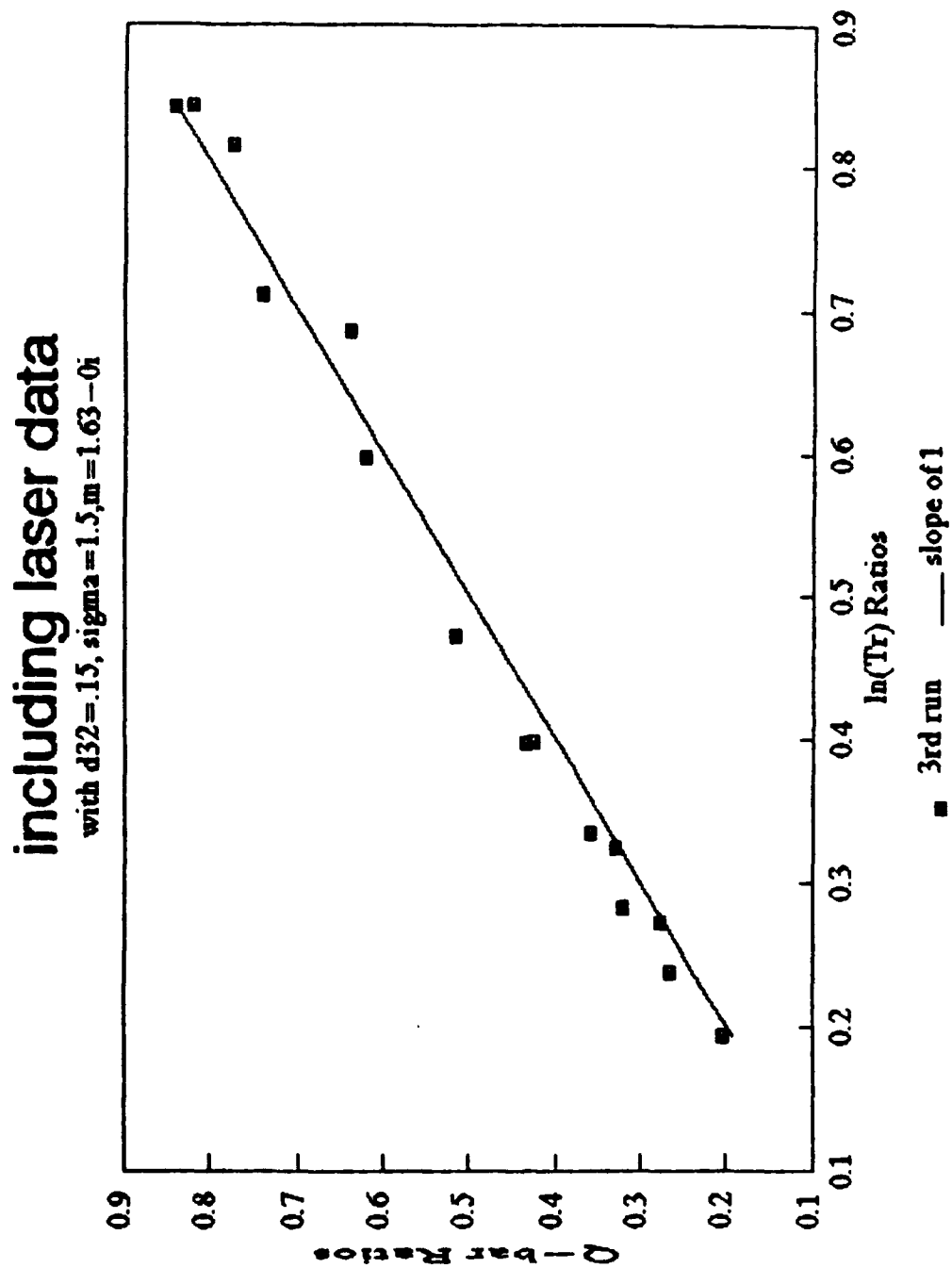


Figure IV-15. Log Transmission vs. Extinction Coefficient Ratios,  
Including  $0.6328 \mu$  Laser Data, Run 3

## V. CONCLUSIONS AND RECOMMENDATIONS

The results of this investigation have shown that the multiple-wavelength light transmission measurement technique can be used to obtain the Sauter mean diameter and standard deviation (of an assumed log-normal size distribution) of the small particles present in the edge of a plume from a solid propellant rocket motor. The technique was shown to be more sensitive to changes in  $d_{32}$  and  $\sigma$  than to  $m$ . The values measured for  $\text{Al}_2\text{O}_3$  in the plume of a small motor using a 4.7% aluminized GAP/AP propellant were  $d_{32} = 0.150 \pm 0.006 \mu$ ,  $\sigma = 1.50 \pm 0.04$  and  $m = 1.63 \pm 0.13$ . The good correlation of the data indicated that only submicron particles were present in the edge of the plume.

Subsequent work should consider the employment of shorter wavelengths in order to provide lower transmittances. This would result in reducing the uncertainties in the log-transmittance ratios which occur when the measured transmittances are high and not adequately separated. This could be accomplished by changing the grating and by using a diode array which has appropriate spectral response in the UV. In addition, more rapid scanning of the diode array would permit a larger number of sweeps to be made in a shorter time. This would reduce the effects of plume fluctuations during the measurements and would provide a larger sample for data averaging.

## APPENDICES

### A. DIODE READINGS

\*\* 1ST RUN W/O PLUME DATA \*\*  
 \*\* DIODE vs. VOLTAGE

210.0	.0035
211.0	.0030
212.0	.0025
213.0	.0035
214.0	.0030
215.0	.0045
216.0	.0045
217.0	.0055
218.0	.0055
219.0	.0045
220.0	.0050
221.0	.0055
222.0	.0035
223.0	.0045
224.0	.0045
225.0	.0055
335.0	.0035
336.0	.0035
337.0	.0035
338.0	.0035
339.0	.0040
340.0	.0035
341.0	.0050
342.0	.0055
343.0	.0055
344.0	.0055
345.0	.0060
346.0	.0050
347.0	.0045
348.0	.0045
349.0	.0045
350.0	.0030
351.0	.0040
352.0	.0035
353.0	.0035
354.0	.0035
432.0	.0025
433.0	.0035
434.0	.0035
435.0	.0040
436.0	.0060
437.0	.0055
438.0	.0055
439.0	.0050
440.0	.0045
441.0	.0055
442.0	.0070
443.0	.0040
444.0	.0050
445.0	.0055
446.0	.0050
447.0	.0050
448.0	.0055
449.0	.0045
450.0	.0035

780.0	.0025
781.0	.0030
782.0	.0030
783.0	.0030
784.0	.0040
785.0	.0035
786.0	.0045
787.0	.0055
788.0	.0050
789.0	.0065
790.0	.0070
791.0	.0055
792.0	.0075
793.0	.0065
794.0	.0040
795.0	.0060
796.0	.0055
797.0	.0060
798.0	.0080
799.0	.0055
800.0	.0045
801.0	.0055
802.0	.0040
803.0	.0045
804.0	.0035
805.0	.0025
806.0	.0040
807.0	.0035
808.0	.0025
809.0	.0030
810.0	.0030
880.0	.0040
881.0	.0035
882.0	.0035
883.0	.0035
884.0	.0040
885.0	.0050
886.0	.0045
887.0	.0050
888.0	.0070
889.0	.0070
890.0	.0060
891.0	.0055
892.0	.0060
893.0	.0070
894.0	.0060
895.0	.0055
896.0	.0070
897.0	.0065
898.0	.0060
899.0	.0055
900.0	.0055
901.0	.0075
902.0	.0065
903.0	.0050
904.0	.0055
905.0	.0035
906.0	.0015
907.0	.0030

XX 1ST RUN WITH PLUME DATA XX

XX DIODE VS. VOLTAGE XX

210.0	.0035	780.0	.0033
211.0	.0027	791.0	.0033
212.0	.0033	782.0	.0040
213.0	.0040	793.0	.0033
214.0	.0043	784.0	.0040
215.0	.0050	795.0	.0042
216.0	.0035	786.0	.0050
217.0	.0018	797.0	.0060
218.0	.0018	788.0	.0065
219.0	.0043	789.0	.0060
220.0	.0049	770.0	.0060
221.0	.0050	791.0	.0063
222.0	.0045	792.0	.0060
223.0	.0040	793.0	.0062
224.0	.0050	794.0	.0060
225.0	.0048	795.0	.0060
226.0	.0035	796.0	.0060
227.0	.0040	797.0	.0065
228.0	.0038	798.0	.0065
229.0	.0045	799.0	.0060
230.0	.0049	800.0	.0062
231.0	.0035	801.0	.0070
232.0	.0038	802.0	.0017
233.0	.0025	803.0	.0038
335.0	.0025	804.0	.0033
336.0	.0025	805.0	.0027
337.0	.0025	806.0	.0030
338.0	.0018	807.0	.0028
339.0	.0045	808.0	.0030
340.0	.0050	809.0	.0033
341.0	.0050	810.0	.0027
342.0	.0040	890.0	.0027
343.0	.0037	881.0	.0018
344.0	.0040	882.0	.0027
345.0	.0030	883.0	.0030
346.0	.0050	884.0	.0047
347.0	.0040	885.0	.0050
348.0	.0045	886.0	.0018
349.0	.0030	887.0	.0047
350.0	.0035	888.0	.0043
351.0	.0043	889.0	.0040
352.0	.0018	890.0	.0060
353.0	.0033	891.0	.0065
354.0	.0045	892.0	.0070
430.0	.0027	893.0	.0065
431.0	.0025	894.0	.0063
432.0	.0027	895.0	.0063
433.0	.0033	896.0	.0050
434.0	.0040	897.0	.0063
435.0	.0043	898.0	.0067
436.0	.0050	899.0	.0057
437.0	.0050	900.0	.0063
438.0	.0053	901.0	.0060
439.0	.0047	902.0	.0038
440.0	.0050	903.0	.0043
441.0	.0048	904.0	.0033
442.0	.0047	905.0	.0023
443.0	.0050	906.0	.0034
444.0	.0050	907.0	.0033
445.0	.0050	908.0	.0035
446.0	.0045	909.0	.0047
447.0	.0043	910.0	.0027
448.0	.0038		
449.0	.0038		
450.0	.0033		

\*\* END RUN WFO PLUME DATA \*\*

\*\* DIODE VS. VOLTAGE \*\*

210.0	.0030	730.0	.0033
211.0	.0027	781.0	.0027
212.0	.0033	782.0	.0030
213.0	.0037	783.0	.0033
214.0	.0037	784.0	.0027
215.0	.0037	785.0	.0037
216.0	.0033	786.0	.0033
217.0	.0043	787.0	.0053
218.0	.0043	788.0	.0050
219.0	.0053	789.0	.0060
220.0	.0040	790.0	.0066
221.0	.0050	791.0	.0067
222.0	.0053	792.0	.0073
223.0	.0053	793.0	.0060
224.0	.0047	794.0	.0063
225.0	.0040	795.0	.0070
226.0	.0047	796.0	.0067
227.0	.0050	797.0	.0063
228.0	.0043	798.0	.0053
229.0	.0043	799.0	.0067
230.0	.0033	800.0	.0057
231.0	.0033	801.0	.0050
232.0	.0030	802.0	.0050
233.0	.0037	803.0	.0043
234.0	.0033	804.0	.0043
235.0	.0047	805.0	.0033
236.0	.0027	806.0	.0043
237.0	.0037	807.0	.0030
238.0	.0030	808.0	.0033
239.0	.0030	809.0	.0023
240.0	.0043	810.0	.0037
241.0	.0040	880.0	.0030
242.0	.0043	881.0	.0030
243.0	.0047	882.0	.0027
244.0	.0053	883.0	.0027
245.0	.0047	884.0	.0027
246.0	.0040	885.0	.0027
247.0	.0047	886.0	.0027
248.0	.0037	887.0	.0047
249.0	.0037	888.0	.0037
250.0	.0043	889.0	.0047
251.0	.0030	890.0	.0060
252.0	.0027	891.0	.0060
253.0	.0037	892.0	.0087
254.0	.0023	893.0	.0057
255.0	.0047	894.0	.0067
256.0	.0027	895.0	.0070
257.0	.0033	896.0	.0067
258.0	.0040	897.0	.0060
259.0	.0033	898.0	.0043
260.0	.0047	899.0	.0050
261.0	.0037	900.0	.0040
262.0	.0043	901.0	.0047
263.0	.0050	902.0	.0023
264.0	.0050	903.0	.0037
265.0	.0060	904.0	.0043
266.0	.0057	905.0	.0027
267.0	.0063	906.0	.0040
268.0	.0053	907.0	.0027
269.0	.0057	908.0	.0037
270.0	.0053	909.0	.0027
271.0	.0047	910.0	.0030
272.0	.0047		
273.0	.0027		
274.0	.0033		

\*\* 2ND RUN WITH PLUME DATA \*\*

\*\* DIODE vs. VOLTAGE\*\*

211.0	.0029	781.0	.0034
212.0	.0035	782.0	.0039
213.0	.0038	783.0	.0045
214.0	.0042	784.0	.0050
215.0	.0045	785.0	.0055
216.0	.0043	786.0	.0058
217.0	.0043	787.0	.0062
218.0	.0050	788.0	.0063
219.0	.0045	789.0	.0060
220.0	.0045	790.0	.0065
221.0	.0045	791.0	.0055
222.0	.0053	792.0	.0055
223.0	.0045	793.0	.0055
224.0	.0035	794.0	.0072
225.0	.0035	795.0	.0055
226.0	.0049	796.0	.0050
227.0	.0040	797.0	.0063
228.0	.0040	798.0	.0060
229.0	.0030	799.0	.0057
230.0	.0030	800.0	.0038
231.0	.0035	801.0	.0045
232.0	.0030	802.0	.0040
233.0	.0033	803.0	.0040
335.0	.0027	804.0	.0033
336.0	.0040	805.0	.0030
337.0	.0030	806.0	.0035
338.0	.0035	807.0	.0025
339.0	.0030	808.0	.0033
340.0	.0035	809.0	.0035
341.0	.0033	810.0	.0027
342.0	.0038	880.0	.0027
343.0	.0035	881.0	.0023
344.0	.0025	882.0	.0025
345.0	.0018	883.0	.0020
346.0	.0043	884.0	.0023
347.0	.0038	885.0	.0030
348.0	.0043	886.0	.0033
349.0	.0033	887.0	.0040
350.0	.0033	888.0	.0043
351.0	.0027	889.0	.0050
352.0	.0030	890.0	.0057
353.0	.0025	891.0	.0058
354.0	.0025	892.0	.0050
430.0	.0025	893.0	.0055
431.0	.0025	894.0	.0060
432.0	.0025	895.0	.0057
433.0	.0033	896.0	.0047
434.0	.0040	897.0	.0053
435.0	.0035	898.0	.0055
436.0	.0040	899.0	.0045
437.0	.0040	900.0	.0039
438.0	.0050	901.0	.0043
439.0	.0050	902.0	.0043
440.0	.0045	903.0	.0033
441.0	.0053	904.0	.0033
442.0	.0053	905.0	.0025
443.0	.0058	906.0	.0022
444.0	.0043	907.0	.0020
445.0	.0040	908.0	.0035
446.0	.0045	909.0	.0023
447.0	.0030	910.0	.0015
448.0	.0033		
449.0	.0040		
450.0	.0033		

3RD RUN W/O PLUME DATA

DIODE VS. VOLTAGE

210.0	.0040
211.0	.0040
212.0	.0050
213.0	.0055
214.0	.0050
215.0	.0050
216.0	.0055
217.0	.0055
218.0	.0055
219.0	.0050
220.0	.0070
221.0	.0055
222.0	.0070
223.0	.0045
224.0	.0060
225.0	.0035
226.0	.0060
227.0	.0040
228.0	.0060
229.0	.0035
230.0	.0045
231.0	.0035
232.0	.0050
233.0	.0040
234.0	.0035
235.0	.0040
236.0	.0040
237.0	.0035
238.0	.0040
239.0	.0040
240.0	.0045
241.0	.0050
242.0	.0050
243.0	.0045
244.0	.0040
245.0	.0030
246.0	.0030
247.0	.0035
248.0	.0040
249.0	.0040
250.0	.0030
251.0	.0040
252.0	.0035
253.0	.0030
254.0	.0030
255.0	.0040
256.0	.0035
257.0	.0035
258.0	.0035
259.0	.0050
260.0	.0050
261.0	.0050
262.0	.0050
263.0	.0050
264.0	.0050
265.0	.0050
266.0	.0050
267.0	.0050
268.0	.0050
269.0	.0050
270.0	.0050
271.0	.0050
272.0	.0050
273.0	.0050
274.0	.0050
275.0	.0050
276.0	.0050
277.0	.0050
278.0	.0050
279.0	.0050
280.0	.0050
281.0	.0050
282.0	.0050
283.0	.0050
284.0	.0050
285.0	.0050
286.0	.0050
287.0	.0050
288.0	.0050
289.0	.0050
290.0	.0050
291.0	.0050
292.0	.0050
293.0	.0050
294.0	.0050
295.0	.0050
296.0	.0050
297.0	.0050
298.0	.0050
299.0	.0050
300.0	.0050
301.0	.0050
302.0	.0050
303.0	.0050
304.0	.0050
305.0	.0050
306.0	.0050
307.0	.0050
308.0	.0050
309.0	.0050
310.0	.0050
311.0	.0050
312.0	.0050
313.0	.0050
314.0	.0050
315.0	.0050
316.0	.0050
317.0	.0050
318.0	.0050
319.0	.0050
320.0	.0050
321.0	.0050
322.0	.0050
323.0	.0050
324.0	.0050
325.0	.0050
326.0	.0050
327.0	.0050
328.0	.0050
329.0	.0050
330.0	.0050
331.0	.0050
332.0	.0050
333.0	.0050
334.0	.0050
335.0	.0050
336.0	.0050
337.0	.0050
338.0	.0050
339.0	.0050
340.0	.0050
341.0	.0050
342.0	.0050
343.0	.0050
344.0	.0050
345.0	.0050
346.0	.0050
347.0	.0050
348.0	.0050
349.0	.0050
350.0	.0050
351.0	.0050
352.0	.0050
353.0	.0050
354.0	.0050
355.0	.0050
356.0	.0050
357.0	.0050
358.0	.0050
359.0	.0050
360.0	.0050
361.0	.0050
362.0	.0050
363.0	.0050
364.0	.0050
365.0	.0050
366.0	.0050
367.0	.0050
368.0	.0050
369.0	.0050
370.0	.0050
371.0	.0050
372.0	.0050
373.0	.0050
374.0	.0050
375.0	.0050
376.0	.0050
377.0	.0050
378.0	.0050
379.0	.0050
380.0	.0050
381.0	.0050
382.0	.0050
383.0	.0050
384.0	.0050
385.0	.0050
386.0	.0050
387.0	.0050
388.0	.0050
389.0	.0050
390.0	.0050
391.0	.0050
392.0	.0050
393.0	.0050
394.0	.0050
395.0	.0050
396.0	.0050
397.0	.0050
398.0	.0050
399.0	.0050
400.0	.0050
401.0	.0050
402.0	.0050
403.0	.0050
404.0	.0050
405.0	.0050
406.0	.0050
407.0	.0050
408.0	.0050
409.0	.0050
410.0	.0050
411.0	.0050
412.0	.0050
413.0	.0050
414.0	.0050
415.0	.0050
416.0	.0050
417.0	.0050
418.0	.0050
419.0	.0050
420.0	.0050
421.0	.0050
422.0	.0050
423.0	.0050
424.0	.0050
425.0	.0050
426.0	.0050
427.0	.0050
428.0	.0050
429.0	.0050
430.0	.0050
431.0	.0050
432.0	.0050
433.0	.0050
434.0	.0050
435.0	.0050
436.0	.0050
437.0	.0050
438.0	.0050
439.0	.0050
440.0	.0050
441.0	.0050
442.0	.0050
443.0	.0050
444.0	.0050
445.0	.0050
446.0	.0050
447.0	.0050
448.0	.0050
449.0	.0050
450.0	.0050

780.0	.0035
781.0	.0035
782.0	.0030
783.0	.0040
784.0	.0050
785.0	.0055
786.0	.0065
787.0	.0060
788.0	.0055
789.0	.0065
790.0	.0065
791.0	.0075
792.0	.0065
793.0	.0070
794.0	.0055
795.0	.0070
796.0	.0060
797.0	.0065
798.0	.0050
799.0	.0050
800.0	.0030
801.0	.0030
802.0	.0025
803.0	.0030
804.0	.0030
805.0	.0040
806.0	.0025
807.0	.0040
808.0	.0030
809.0	.0040
810.0	.0025
811.0	.0025
812.0	.0025
813.0	.0025
814.0	.0025
815.0	.0025
816.0	.0025
817.0	.0025
818.0	.0025
819.0	.0025
820.0	.0025
821.0	.0025
822.0	.0025
823.0	.0025
824.0	.0025
825.0	.0025
826.0	.0025
827.0	.0025
828.0	.0025
829.0	.0025
830.0	.0025
831.0	.0025
832.0	.0025
833.0	.0025
834.0	.0025
835.0	.0025
836.0	.0025
837.0	.0025
838.0	.0025
839.0	.0025
840.0	.0025
841.0	.0025
842.0	.0025
843.0	.0025
844.0	.0025
845.0	.0025
846.0	.0025
847.0	.0025
848.0	.0025
849.0	.0025
850.0	.0025
851.0	.0025
852.0	.0025
853.0	.0025
854.0	.0025
855.0	.0025
856.0	.0025
857.0	.0025
858.0	.0025
859.0	.0025
860.0	.0025
861.0	.0025
862.0	.0025
863.0	.0025
864.0	.0025
865.0	.0025
866.0	.0025
867.0	.0025
868.0	.0025
869.0	.0025
870.0	.0025
871.0	.0025
872.0	.0025
873.0	.0025
874.0	.0025
875.0	.0025
876.0	.0025
877.0	.0025
878.0	.0025
879.0	.0025
880.0	.0025
881.0	.0025
882.0	.0025
883.0	.0025
884.0	.0025
885.0	.0025
886.0	.0025
887.0	.0025
888.0	.0025
889.0	.0025
890.0	.0025
891.0	.0025
892.0	.0025
893.0	.0025
894.0	.0025
895.0	.0025
896.0	.0025
897.0	.0025
898.0	.0025
899.0	.0025
900.0	.0025
901.0	.0025
902.0	.0025
903.0	.0025
904.0	.0025
905.0	.0025
906.0	.0025
907.0	.0025
908.0	.0025
909.0	.0025
910.0	.0025



\*\* 3RD RUN WITH PLUME DATA \*\*

\*\* DIGDE vs. VOLTAGE\*\*

210.0	.0023	780.0	.0030
211.0	.0023	781.0	.0027
212.0	.0033	782.0	.0030
213.0	.0037	783.0	.0033
214.0	.0023	784.0	.0037
215.0	.0030	785.0	.0040
216.0	.0037	786.0	.0047
217.0	.0043	787.0	.0040
218.0	.0053	788.0	.0037
219.0	.0043	789.0	.0053
220.0	.0010	790.0	.0020
221.0	.0050	791.0	.0053
222.0	.0050	792.0	.0050
223.0	.0043	793.0	.0060
224.0	.0040	794.0	.0050
225.0	.0040	795.0	.0067
226.0	.0053	796.0	.0057
227.0	.0047	797.0	.0037
228.0	.0047	798.0	.0050
229.0	.0027	799.0	.0053
230.0	.0030	800.0	.0050
231.0	.0036	801.0	.0047
232.0	.0050	802.0	.0043
233.0	.0033	803.0	.0043
234.0	.0030	804.0	.0037
235.0	.0033	805.0	.0030
236.0	.0030	806.0	.0030
237.0	.0037	807.0	.0027
238.0	.0030	808.0	.0027
239.0	.0037	809.0	.0030
240.0	.0040	810.0	.0027
241.0	.0047	811.0	.0027
242.0	.0033	812.0	.0030
243.0	.0043	813.0	.0027
244.0	.0037	814.0	.0027
245.0	.0040	815.0	.0033
246.0	.0050	816.0	.0040
247.0	.0040	817.0	.0037
248.0	.0033	818.0	.0033
249.0	.0030	819.0	.0040
250.0	.0030	820.0	.0040
251.0	.0033	821.0	.0043
252.0	.0037	822.0	.0060
253.0	.0037	823.0	.0057
254.0	.0033	824.0	.0060
255.0	.0030	825.0	.0067
256.0	.0033	826.0	.0063
257.0	.0033	827.0	.0063
258.0	.0037	828.0	.0057
259.0	.0030	829.0	.0057
260.0	.0037	830.0	.0050
261.0	.0047	831.0	.0047
262.0	.0053	832.0	.0043
263.0	.0047	833.0	.0047
264.0	.0050	834.0	.0033
265.0	.0057	835.0	.0030
266.0	.0047	836.0	.0030
267.0	.0043	837.0	.0030
268.0	.0037	838.0	.0033
269.0	.0043	839.0	.0027
270.0	.0040	840.0	.0030
271.0	.0037	841.0	.0030
272.0	.0030	842.0	.0030
273.0	.0030	843.0	.0030
274.0	.0030	844.0	.0030
275.0	.0030	845.0	.0030
276.0	.0030	846.0	.0030
277.0	.0030	847.0	.0030
278.0	.0030	848.0	.0030
279.0	.0030	849.0	.0030
280.0	.0030	850.0	.0030

## B. DATA ACQUISITION PROGRAM

```

20 ***** ACQUIRES MULTIPLE SCANS OF P-N DIODE ARRAYS *****
30 ***** AND STORES THEM ON DISK *****
40 ***** HANSEN, KELLY HARRIS, KIM HONG-ON 1991 *****
50 OPTION PAGE 1
60 COM Q1:[12],Q2:[12],T1:[20],D1:[12],D2:[12],Address(4),E(4076)
70 COM A(1024) PUFFER,B(4096) BUFFER,C(4096) BUFFER,D(4096) BUFFER
80 ASSIGN SMult110 TO 72310 ! CLEARS THE WAKE-UP SERVICE REQUEST
90 ENTER SMult110;Qq1,Qq2,Qq3,Qq4,Qq5,Qq6 ! OF THE MULTIPROGRAMMER
100 MAT Address= (0) ! ZEROS THE ARRAY FOR DEBUGGING
120 LOCAL LOCKOUT 7 ! DISABLES FRONT PANELS OF DATA ACQUISITION SYSTEM
130 REMOTE 709
140 OUTPUT 707;"AR" ! ANALOG RESET OPENS ALL CHANNELS
160 REMOTE 722 ! REMOTE IS A LISTEN COMMAND
170 OUTPUT 722;"HSM002S01D1L1Z0F1FLOP11STN.01ST113Q" ! PROGRAM VOLTMETER
180 ! H hones the DVM (like RESET) SM002 sets the service request mask to
190 ! tell the computer that a measurement was taken and is ready to be read.
200 ! page 3-20 of DVM MANUAL. SC1 means that no reading will be taken until
210 ! the computer receives the one just made (page 3-26). D1 means DISPLAY ON.
220 ! L1 means load the following instructions. Z0 means AUTO ZERO OFF for
230 ! faster but less precise readings. F1 means DC VOLTS measurement.
240 ! FLO means FILTER OFF for faster readings. R1 is AUTO RANGING. 1STN means
250 ! 1 reading will be taken for each trigger. .01ST1---.01powerline cycles
260 ! will be the integration time. T3 is a single trigger. Q means END
270 PRINT USING "3/"
280 PRINT "ENTER THE FILENAMES OF THE DATA FILES TO BE CREATED (e.g. RAW1,RAW2)"
290 PRINT "12 CHARACTERS MAXIMUM, EACH"
300 PRINT USING "/"
310 PRINT "AN EMPTY DISK MUST BE IN THE LEFT DISK DRIVE"
320 PRINT ""
330 PRINT "THE DATA FILES WILL NEARLY FILL A DISK"
340 PRINT USING "/"
350 MASS STORAGE IS ":CS80,700" ! CHANGE THIS LATER IF NECESSARY
360 INPUT "INPUT FILE NAMES NOW - (FILENAME1,FILENAME2) ",D1$,D2$
370 M5=1024
380 Zz$="INTERNAL,4,1" ! STRING INDICATES MASS STORAGE
390 CREATE BDAT D1$Zz$,6144,16 ! 12 SCANS OF 1024 @ 2*8 BYTES PER RECORD
400 CREATE BDAT D2$Zz$,6144,16 ! 1024*12/2=NUMBER OF RECORDS=6144
410 PRINT USING "E"
420 PRINT "DATA WILL BE STORED ON DISKETTE WITH FOLLOWING FILE NAMES:"
430 PRINT USING "///"
440 PRINT "NO PARTICLES ---- FILENAME = ";D1$
450 PRINT "PARTICLES ----- FILENAME = ";D2$
460 OUTPUT 709;"DC11,2" ! OPEN SHUTTER
470 PRINT USING "///"
480 PRINT "IS THIS A CALIBRATION ? ENTER Y / IF YES"
490 INPUT R$
500 PRINT USING "///"
510 PRINT "BE SURE LASER IS ON"
520 PRINT "PRESS (CONTINUE) WHEN READY"
530 PAUSE
540 IF R$="Y" THEN 740
550 PRINT USING "E"
560 INPUT "ENTER THE TRIGGER VOLTAGE",V1
570 OUTPUT 709;"AC20" ! CHANNEL FOR CHAMBER PRESSURE
580 WAIT .3 ! THIS WAIT IS TO LET VOLTAGES SETTLE DOWN
590 V1=0
600 CLEAR 722 ! THIS DOES NOT ALTER THE INSTRUCTIONS FOR THE VOLTMETER
610 ! IT CLEARS ANY NUMBERS IN THE DISPLAY OR OUTPUT REGISTERS
620 FOR I=1 TO 10
630 OUTPUT 722;"X1" ! TRIGGER VOLTMETER
640 GOSUB Reading ! READ VOLTMETER
650
660

```

```

670 V1=V1+V
680 NEXT I
690 V2=V1/10      ! THIS AVERAGES READINGS TO GET A ZERO PRESSURE VALUE
700 PRINT USING " 40A,0.60"; V2      ! ZERO PRESSURE VOLTAGE IS V2
710 PRINT
731 PRINT " DATA ACQUISITION BEGINS WHEN VOLTAGE EXCEEDS V1
740 D3=D14      ! NO-PARTICLES STRING NAME
750 GOSUB Multiprog      ! TAKES NO-PARTICLE DATA
760 GOSUB Storedata
770 IF P$="" THEN 960      ! IF CALIBRATION THEN SKIP SOME LINES
780 PRINT USING "/"
790 PRINT " BE SURE NITROGEN IS ON"
800 PRINT "BE SURE VISICORDER IS SET UP TO RUN ON PROPER SCALE WITH LAMP ON."
810 PRINT USING "/"
820 DISP "      STANDING BY FOR IGNITION"
830 PRINT "      STANDING BY FOR IGNITION"
840 BEEP 2000,1
850 OUTPUT 709;"AC20"      ! CONNECT PRESSURE ADUCER TO DVM
860 CLEAR 722
870 WAIT .3
880 OUTPUT 722;"X1"      ! TRIGGER VOLTMETER
890 GOSUB Reading
900 R9=ABS(V-V2)      !THIS IS VOLTAGE CORRESPONDING TO PRESSURE
910 PRINT R9
920 IF R9<V1 THEN GOTO 830 : IF PRESSURE IS BELOW THRESHOLD PRESSURE--REPEAT
931 DISP ""
930 Q0=TIME$
940 WAIT T0=.13      ! ALLOWS FOR .13 SECONDS TO PROGRAM MEMORY CARDS
950 IF R9<V1 THEN 1020      !IF ACTUAL RUN THEN SKIP SOME LINES
960 ! FOR CALIBRATIONS INTRODUCE PARTICLES AND THEN CONTINUE
970 PRINT CHR$(12)
980 PRINT USING "/////////"
990 PRINT "      INTRODUCE PARTICLES THEN PRESS KEY # 9 TO TAKE DATA"
1000 ON KEY 9 LABEL " TAKE DATA" GOTO 1020
1010 Standby: GOTO Standby
1020 GOSUB Multiprog      ! TAKE PARTICLE DATA
1030 D3=D2$      !PARTICLE DATA FILE NAME
1040 GOSUB Storedata
1050 PRINT "ELAPSED TIME FROM PRESSURE TO END OF TIME DELAY";DROUND(D1-Q0,3)
1070 PRINT "ELAPSED TIME FROM START TO END OF DATA ACQUISITION";DROUND(Q2-Q1,3)
1080 PRINT " DATA STORED ON DISK WITH FILENAMES (";D1$;) AND (";D2$;)"
1081 OUTPUT 709;"AR"
1082 LOCAL 7
1090 GOTO End
1100 Multiprog: !
1101 OUTPUT 709;"DC16,6"
1102 OUTPUT 709;"D310,3"
1110 OUTPUT 723;"CC,2,3,12,13T"
1120 OUTPUT 723;"CC,5,6,7,10T" !CLEARS THE ARM,BUSY AND EOP OF MEMORY CARDS
1130 OUTPUT 723;"CC,1,4,11T" !CLEARS SAME FOR A TO D'S AND TIMER PACER
1140 OUTPUT 723;"SF,2,3,1,.001,12,T" ! THE .1) IS 2'S COMPLIMENT BINARY
1150 OUTPUT 723;"SF,5,3,1,.001,12,T" ! THE .001 IS THE LEAST SIGNIFICANT BIT
1160 OUTPUT 723;"SF,9,3,1,.001,12,T" ! THE 12 IS FOR 12 BIT WORD SIZE
1170 OUTPUT 723;"SF,12,3,1,.001,12,T" ! SINCE THE A TO D IS 12 BIT
1180 OUTPUT 723;"WF,3,1023T,WF,6,4095T"
1190 OUTPUT 723;"WF,10,4095T,WF,13,4095T"
1200 ! SETS REFERENCE WORD FOR WHEN TO STOP TAKING DATA AND GENERATE INTERRUPT
1210 OUTPUT 723;"WF,2,1,21T,WF,5,1,21T" !SETS FIFO MODE
1211 OUTPUT 723;"WF,7,1,1T,WF,12,1,1T"
1220 OUTPUT 723;"WF,3,1,0T,WF,3,2,0T,WF,3,3,0T,WF,13,1,0T,WF,13,2,0T,WF,13,3,0T"
1230 OUTPUT 723;"WF,6,1,0T,WF,6,2,0T,WF,6,3,0T,WF,10,1,0T,WF,10,2,0T,WF,10,3,0T"
1240 ! SETS COUNTER AND POINTERS OF 2ND MEMORY CARD IN EACH PAIR TO 0
1250 OUTPUT 723;"AC,2T,AC,5T,AC,9T,AC,12T" !ARMS CARDS WHICH GENERATE INTERRUPT
1260 OUTPUT 723;"AC,3T,AC,5T,AC,10T,AC,13T"
1270 Q1=TIME$
1280 OUTPUT 723;"WF,4,2,0T,WF,4,2ST" ! TIMER PACER GIVES 1 PULSE OF 1 SEC WHEN
1290 ! TRIGGERED BY THE BLANKING PULSE (PLENTY OF TIME FOR 8 SCANS)

```

```

1291 WAIT 3
1300 !MAY NOT NEED ANY WAIT LONGER THAN .5 SECONDS FOR ALL CARDS TO FILL
1301 OUTPUT 723;"WF,2,1,1T,WF,5,1,1T" !ENABLE THE MEMORY CARD
1302 OUTPUT 709;"DC10,3"
1303 OUTPUT 709;"DO11,2"
1304 OUTPUT 709;"DO10,5"
1305 WAIT 2
1306 !WAIT FOR MEM INTERRUPT
1310 K=SPOLL(723)
1320 IF K(264) THEN GOTO 1310
1330 OUTPUT 723;"WF,4,2,1T" !MAY BE UNNECESSARY TO ALTER TIMER PACER SINCE
1340 !MEMORY CARDS HAVE AUTOMATIC LOCKOUT BUT FOR NOW WE WILL DO IT
1350 Q2=TIMEDATE
1351 OUTPUT 709;"DO11,2"
1360 ON ERROR GOTO Err_trap !NEEDED TO READ ARMED CARD INTERRUPT LIST
1370 SEND 7;UM;M.A TALK 23 SEC 12 !SPECIFICALLY ASKS FOR INTERRUPT LIST
1380 Var read: ENTER 7;address(4) !READ WHICH CARDS INTERRUPTED
1390 memcards: PRINT "MEMORY CARDS WHICH GENERATED INTERRUPTS ARE "
1400 PRINT "SLOTS# = ",address(*)
1410 MAT Address= (0)
1420 OFF ERROR
1430 OUTPUT 723;"DC,3,6,13,10T" !DISSARM MEM CARDS
1440 OUTPUT 723;"MI,2,1024T" !SET UP CARD TO BE READ
1450 ENTER 72305;A(4) !GETS DATA FROM 1024 MEMORY BOARD
1460 OUTPUT 723;"MI,5,4096T"
1470 ENTER 72305;B(4) !GETS DATA FROM 4096 MEMORY BOARD
1480 PRINT "EXHAUST DATA ENTERED"
1490 OUTPUT 723;"MI,12,4096T"
1500 ENTER 72305;C(4)
1510 OUTPUT 723;"MI,9,4096T"
1520 ENTER 72305;D(4)
1530 ENABLE INTR 7,8
1540 PRINT "MOTOR DATA ENTERED"
1550 MAT A= (-1)*A !THE 1024 CARD IS INCLUDED BUT NOT SAVED. IT DIDN'T
1560 MAT B= (-1)*B !PERFORM WELL. COULD BE REPLACED BY A 4096 CARD.
1570 MAT C= (-1)*C
1580 MAT D= (-1)*D !SINCE VOLTAGES ARE NEGATIVE SO SIGNS ARE CHANGED
1590 RETURN
1600 Stop:Data:
1610 ASSIGN $Diskfile TO $DiskZz
1620 ASSIGN $B:FF1 TO BUFFER C(4) !MOTOR CAVITY 4 SCANS
1630 ASSIGN $B:FF2 TO BUFFER D(4) !MOTOR CAVITY 4 SCANS
1640 ASSIGN $B:FF3 TO BUFFER E(4) !EXHAUST 4 SCANS
1650 CONTROL $B:FF1,3,1,32768,1 !SETS BUFFER POINTERS TO FULL
1660 CONTROL $B:FF2,3,1,32768,1 !INTERFACE REGISTERS SECTION OF
1670 CONTROL $B:FF3,3,1,32768,1 !LANGUAGE MANUAL
1680 TRANSFER $B:FF1 TO $Diskfile !ORDER OF DATA ON THE DISK IS
1690 WAIT FOR EOT $Diskfile !MOTOR CAVITY--6 SCANS
1700 TRANSFER $B:FF2 TO $Diskfile !EXHAUST -- 4 SCANS
1710 WAIT FOR EOT $Diskfile !WAIT BECAUSE OVERLAPPING
1720 TRANSFER $B:FF3 TO $Diskfile !TRANSFERS ARE NOT WANTED
1730 WAIT FOR EOT $Diskfile
1740 ASSIGN $Diskfile TO *
1750 ASSIGN $B:FF1 TO *
1760 ASSIGN $B:FF2 TO *
1770 ASSIGN $B:FF3 TO *
1780 RETURN
1790 Read vol:
1800 ENTER 722,0 !READS VOLTMETER
1810 RETURN
1820 Err_trap: IF ERR#157 AND ERR(Var read) THEN memcards
1830 PRINT ERR# !IF THE ERROR WAS NOT THE ONE PLANNED
1840 GOTO memcards !FOR PROGRAM EXECUTION CONTINUES
1850 OUTPUT 723;"DO,0,15" !THIS ACTIVATES THE HALVERN EXT TRIGGER (VOLTS = 5)
1860 PRINT "TAKING DATA WITH HALVERN"
1870 WAIT 3
1880 PRINT "RESETTING HALVERN"
1890 OUTPUT 709;"DO10,15"
1899 PRINT "RUN COMPLETED WITH HALVERN ONLY DATA"
1900 END:END

```

## REFERENCES

1. Netzer, D. W., *Tactical Missile Propulsion-Design and Applications*, Unpublished Course Notes, Naval Postgraduate School, 1991.
2. Dash, S. M., *Analysis of Exhaust Plumes and Their Interaction with Missile Airframes*, A.I.A.A. Progress in Astronautics and Aeronautics, Vol. 104, Tactical Missile Aerodynamics, pp. 778-851.
3. Hwang, C. J. and Chang, G. C., *Numerical Study of Gas-Particle Flow in Solid Rocket Nozzle*, AIAA J., Vol. 26, No. 6, June 1988, pp. 682-689.
4. Lyons, R. B., Wormhoudt, J. and Gruninger, J., *Scattering of Radiation by Particles in Low Altitude Plumes*, AIAA-81-1053, AIAA 16<sup>th</sup> Thermophysics Conference, June 1981, Palo Alto, CA.
5. Cashdollar, K. L., Lee, C. K. and Singer, J. M., *Three-Wavelength Light Transmission Technique to Measure Smoke Particle Size and Concentration*, Applied Optics, Vol. 18, No. 11, June 1979, pp. 1763-1769.
6. Mie A. F. W. L, Gustav, *Contributions to the Optics of Cloudy Media, Especially of Colloidal Metallic Solutions*, Ann. Physik 4th series, 25:3:377-445, 1908.
7. Dobbins, R. A., and Jizmagian, J., *Particle Measurements Based on Use of Mean Scattering Cross-section*, Opt. Soc. Am., Vol. 56, No. 10, pp 1351-1354, 1966.
8. Rosa, J. S., *Particle Sizing in a Solid Propellant Rocket Motor Using Scattered Light Measurements*, Master's Thesis, Naval Postgraduate School, Monterey, California, December 1985.
9. Oriel Corp., *Light Sources*, Oriel Catalog, Volume II, Strafford, CT.
10. EG & G Reticon, *Spectral Response of Reticon Linear Photodiode Arrays*, Application Notes, No.121, Sunnyvale, California.
11. Harris, R. K., *An Apparatus for Sizing Particulate Matter in Solid Rocket Motors*, Master's Thesis, Naval Postgraduate School, Monterey, California, June 1984.

12. Lotus Corp., *Lotus123, Release 3.1*, pp 2-70 - 2-74, Cambridge, Massachusetts.
13. Spiegel, M. R., *Probability and Statistics*, McGraw Hill, pp 263-265, 1990.

## INITIAL DISTRIBUTION LIST

	NO. Copies
1. Defence Technical Information Center Cameron Station Arlington, Virginia 22304-6145	2
2. Library, Code 52 Naval Postgraduate School Monterey, California 93943-5002	2
3. Department Chairman, Code AA Department of Aeronautics Naval Postgraduate School Monterey, California 93943-5000	1
4. Professor D. W. Netzer, Code AA/Nt Department of Aeronautics Naval Postgraduate School Monterey, California 93943-5000	2
5. David Laredo, Code AA Department of Aeronautics Naval Postgraduate School Monterey, California 93943-5000	1
6. Major Kim, Hong-on 839-4 Bokdae-Dong Cheongju-Shi Seoul Korea 360-270	5